American Mineralogist, Volume 77, pages 1050–1066, 1992

Fluid fugacities and phase equilibria in the Fe-Si-O-H-S system

Pingfang Shi

Planetary Geochemistry Program, Department of Mineralogy and Petrology, Box 555, Uppsala University, S-751 22, Uppsala, Sweden

Abstract

By applying the model for C-H-O-S multicomponent fluids (Saxena and Fei, 1987a, 1987b, 1988a, 1988b; Shi and Saxena, 1992), a series of pressure-temperature calibrations of several f_{O_2}-f_{H_2}-f_{S_2} buffers have been established, including hematite + magnetite, fayalite + quartz + magnetite, fayalite + quartz + Fe, magnetite + Fe, wüstite + magnetite, wüstite + Fe, pyrrhotite + pyrite, pyrrhotite + Fe, pyrrhotite + pyrite + magnetite, hematite + magnetite + pyrite, fayalite + quartz + magnetite + pyrrhotite, fayalite + quartz + Fe + pyrrhotite, magnetite + Fe + pyrrhotite/wüstite + Fe + pyrrhotite/wüstite + magnetite + pyrrhotite, and hematite + pyrite + $FeSO_4$. The theoretically calculated phase diagrams are consistent with the available experimental data within uncertainties. Phase equilibria and fluid proportions of various species in the Fe-Si-O-H-S system are calculated.

Introduction

Theoretical and experimental investigations of chemical equilibria and kinetics in the carbonate-silicate-oxide-sulfide-fluid system have been widely made in modern geochemical studies and industrial research. The knowledge of heterogeneous equilibria in the Fe-Si-O-H-S system is a prerequisite to an understanding of the redox conditions, fluid fugacities, and phase relationships in many geological systems.

The application of O-buffer techniques brought a revolution to experimental mineralogy, petrology, and geochemistry. Eugster and coworkers (e.g., Eugster, 1957; Eugster and Wones, 1962; Wones and Gilbert, 1969; Williams, 1971; Chou, 1978, 1986; Hewitt, 1978; Myers and Eugster, 1983; Chou and Cygan, 1990; Ulmer and Luth, 1991) pioneered the study of the redox conditions in the Fe-Si-O-H system and applied the results to understand the chemical equilibria in hydrothermal systems. In the S-bearing systems, some anhydrous and hydrothermal studies were undertaken to study sulfidation reactions (e.g., Arnold, 1958, 1962; Barton and Toulmin, 1964, 1966; Toulmin and Barton, 1964; Giletti et al., 1968; Schneeberg, 1973; Craig and Scott, 1974; Gamble, 1978, 1982; Burton et al., 1982; Kissin and Scott, 1982; Spry and Scott, 1986; Janecky et al., 1986; Wood et al., 1987). Recently, Kishima and Sakai (1984) and Kishima (1986, 1989) developed a hydrothermal analytical technique to determine several fluid fugacities simultaneously. Although there are many different experimental methods used in calibrating the relationships among f_{O_2}-f_{H_2}, temperature, pressure, and Fe^{2+}/Fe^{3+} ratios in silicate oxides (solids or melts), the applicable ranges of all buffers are limited to low temperatures and low pressures. Furthermore, large discrepancies among various experiments prohibit potential applications. To date a complete theoretical calculation of the relationships among temperature, pressure, and f_{O_2}-f_{H_2}-f_{CO_2}-f_{CH_4}-f_{S_2} in the Fe-Si-C-H-O-S system has not been done. The introduction of the C-H-O-S multicomponent fluid model (Shi and Saxena, 1992) along with the improvements in thermodynamic properties of minerals (Saxena et al., 1992; Holland and Powell, 1990) and in free energy minimization programs (e.g., Eriksson, 1975; Saxena and Eriksson, 1985; Sundman et al., 1985; Sundman, 1991) make it possible for us to calculate fluid fugacities and phase equilibria in carbonate-silicate-oxide-sulfide-fluid systems in the crustal temperature-pressure range from critical points up to 2000 °C and 20 kbar. This study was performed to investigate the fluid fugacities of various $f_{O_2}+f_{H_2}+f_{S_2}$ buffers and phase equilibria in the Fe-Si-H-O-S system.

Thermodynamic consideration and assessment

The Gibbs free energy of a compound at a temperature of T (K) and a pressure of P (bar) is given by $G^0_{P,T} = H^0_T - TS^0_T + \int_1^P V\,dP$, where H^0_T and S^0_T are the standard enthalpy and entropy of a compound at T (K) and 1 bar, respectively, obtained from $H^0_T = H^0_{f,1,298.15} + \int_{298}^T C_P/T\,dT$ and $S^0_T = S^0_{1,298.15} + \int_{298}^T (C_P/T)\,dT$. The formulation of heat capacity C_P chosen in this study is as follows (Saxena et al., 1992): $C_P = a + bT + cT^{-2} + dT^2 + eT^{-3} + fT^{-1/2} + gT^{-1}$.

For C-H-O-S fluid species, Shi and Saxena (1992) provide an effective and reliable model to calculate thermodynamic properties for both pure fluid species and fluid mixtures over the crustal temperature-pressure range from critical points up to 2000 °C and 20 kbar.

For pure solid phases, molar volume as a function of

0003–004X/92/0910–1050$02.00

temperature and pressure $V(P,T)$ can be calculated according to the Murnaghan equation (e.g., Saxena et al. 1992)

$$V(P,T) = V(1,T)\left(1 + \frac{K_T'' P}{K_0 + K_T'(T - 298.15)}\right)^{-[K_T'']^{-1}} \quad (1)$$

where K_0 is the isothermal bulk modulus at 298.15 °C, K_T' and K_T'' are its temperature and pressure derivatives, $(\partial K_T/\partial T)_P$ and $(\partial K_T/\partial P)_T$, respectively. $V(1,T)$ is the molar volume at T and 1 bar given by $V(1,T) = V^0_{298}$ $[1 + \int_{298}^{T} \alpha(T)\, dT]$, where V^0_{298} is the molar volume at 298.15 K and 1 bar, and $\alpha(T)$ is the thermal expansion defined as $\alpha(T) = \alpha_0 + \alpha_1 T + \alpha_2 T^{-2}$. Therefore, the contribution of $V(P,T)$ to the Gibbs free energy is given by

$$\int_1^P V(P,T)\, dP = V^0_{298}\left[1 + \alpha_0(T - 298.15) + \frac{\alpha_1}{2}(T^2 - 298.15^2) - \alpha_2\left(\frac{1}{T} - \frac{1}{298.15}\right)\right] \times \left\{\frac{K_0 + K_T'(T - 298.15)}{K_T'' - 1} \times \left[\left(1 + \frac{K_T'' P}{K_0 + K_T'(T - 298.15)}\right)^{(K_T'' - 1)/K_T''} - 1\right]\right\}. \quad (2)$$

Thermodynamic properties of solid phases in the Fe-Si-O-H-S system are listed in Table 1. Barring the S-bearing phases, all other data for solid phases have been systematized by Saxena et al. (1992) from the available thermochemical and phase equilibrium data (Mao et al., 1967, 1974; Liebermann and Schreiber, 1968; Robie et al., 1978, 1982; Barin and Knacke, 1978; Saxena and Eriksson, 1983; Haas, 1988; Akimoto et al., 1976; Saxena et al., 1986; Fei and Saxena, 1986; Chatterjee, 1987, 1989; Hemingway, 1990; Fei et al., 1990).

The C_P expressions for pyrrhotite and pyrite and the standard enthalpy and entropy of pyrrhotite ($Fe_{0.877}S$) are assessed in this study based on the C_P data given in JANAF (1985), Mills (1974), and Robie et al. (1978) and phase equilibria involving pyrrhotite, pyrite, sphalerite, and fluids. The standard enthalpy of formation for $Fe_{1-x}S$ was previously studied by Ariya et al. (1966), Bugli et al. (1972), Stolyarova and Bezman (1976), among others, using different methods such as solution calorimetry, reaction calorimetry, and the third law evaluation (see Mills, 1974; JANAF, 1985). According to Ariya et al. (1966) and Bugli et al. (1972), the relationship between ΔH_f^0 and N_{FeS} is complicated, and one cannot easily express ΔH_f^0 as a function of N_{FeS}. The values of ΔH_f^0 for pyrrhotite with composition between $N_{FeS} = 0.9000$–1.000 were chosen to be the same as those for $Fe_{0.877}S$ (i.e., the Fe-site vacancy $x = 0.123$ or $N_{FeS} = 0.9345$ in the FeS-□S solid solution). This value was assessed in this study (−99440.0 J/mol), and it lies between that of Bugli et al. (1972, −92413.4 J/mol) and of JANAF (1985, −106310.0 J/mol). The effect of composition on the molar volume of pyrrhotite, as given by Toulmin and Barton (1964), Scott (1973), Craig and Scott (1974), and Froese and Gunter (1976), $V = V_0 + 1.841N_{FeS}$, is very small, decreasing by about 0.52% from $N_{FeS} = 1$ to 0.95 or 0.90 by 0.84% to 0.90, respectively.

The solid solutions in this system include wüstite (FeO-$FeO_{1.5}$) and pyrrhotite (FeS-□S). The excess free energy for a binary system is given by

$$G_m^{ex} = X_1 X_2 (W_{21} X_1 + W_{12} X_2) \quad (3)$$

where W_{ij}'s are interaction energy parameters. For ternary and quaternary or higher-order systems, the Solgasmix program calculates the ternary and quaternary or higher-order interaction energies based on the Kohler model (see Saxena and Eriksson, 1983, 1986).

The calculation of the f_{O_2}-f_{H_2}-f_{S_2} buffers

The calculations of f_{O_2}-f_{H_2}-f_{S_2} buffers were performed by using the modified version of the program Solgasmix (Eriksson, 1975) for a system involving both solid solutions and fluid mixture. The calculations have been performed by considering both thermal expansion (α) and bulk modulus (K). Since in the range of P and T of interest, the inclusion of these effects on volume of solids has no significant effect, the data on α and K are not listed in Table 1. The program uses the method of free energy minimization as discussed by Saxena and Eriksson (1983, 1985, 1986). Table 2 summarizes the invariant and univariant buffering reactions and divariant nonbuffering reactions involved in this study. Both abbreviated names (the first column in Table 2) and the normal abbreviations (the second column, under "pure") will be used for convenience and simplicity in either text or figures. The buffer + H_2O equilibrium assemblages are implied by the W included in the abbreviations (the third column, under "with H_2O"). By "invariant," "univariant," or "divariant" reaction, we mean in the f_{O_2}-f_{S_2} space the reaction has zero, single, or double degree of freedom at fixed temperatures and pressures in the Fe-Si-O-H-S system. The thermal expansion (α) and bulk modulus (K) for solid phases and the calculated f_{O_2} and f_{H_2} values for the f_{O_2} buffers (Hm + Mt, Fay + Qtz + Mt, Fay + Qtz + Fe, Mt + Fe, Wüs + Fe, Wüs + Mt) are given in Appendixes 1 and 2.[1]

Hm + Mt f_{O_2} buffer

The HM (hematite + magnetite) equilibrium has been determined experimentally by Darken and Gurry (1945, 1946), Chou (1978), Myers and Eugster (1983), and Kishima and Sakai (1984) and thermodynamically calculated by Eugster and Wones (1962), Haas and Robie

[1] To obtain a copy of Appendixes 1 and 2, order Document AM-92-508 from the Business Office, Mineralogical Society of America, 1130 Seventeenth Street NW, Suite 330, Washington, DC 20036, U.S.A. Please remit $5.00 in advance for the microfiche.

TABLE 1. Thermodynamic properties of some solid phases in the Fe-Si-O-H-S system*

No.	Phase name	Abb.	Formula	$\Delta H^0_{f,1,298}$ (J/mol)	$S^0_{1,298}$ (J/mol·K)	$V^0_{1,298}$ (cm³/mol)
1	Quartz	Qtz	SiO_2	−910 700.0	41.460	22.690
2	Fe (BCC)	Fe	Fe	0.0	27.280	7.150
3	Fayalite	Fay	½(Fe_2SiO_4)	−739 085.0	75.500	23.140
4	Clinoferrosilite	Fs	½($Fe_2Si_2O_6$)	−1 193 590.0	95.400	33.140
5	Magnetite	Mt	¼(Fe_3O_4)	−278 739.0	37.560	11.131
6	Hematite	Hm	½(Fe_2O_3)	−412 795.0	44.030	15.137
7	Wüstite (1)	Wüs	FeO	−267 270.0	57.590	12.250
8	Wüstite (1.5)	Wüs	$FeO_{1.5}$	−380 900.0	54.900	15.970
9	Pyrrhotite	Po	$Fe_{0.877}S$	−99440.0	60.799	17.580
10	Pyrite	Py	FeS_2	−171 544.0	52.930	23.940
11	Ferrous sulfate	$FeSO_4$	$FeSO_4$	−919 330.0	120.957	50.633

$C_P(T)$**

$C_P(T) = a + bT + cT^{-2} + dT^2 + eT^{-3} + fT^{-0.5} + g/T$

No.	T_{tr} (K)	ΔH_{tr} (J/mol)	a (10^2)	b (10^{-3})	c (10^6)	d (10^{-6})	e (10^8)	f	g (10^4)
1			1.01490	2.782	4.353	0.0	−1.913	0.0	−2.961
	848	0.0	0.62684	21.039	−2.5826	0.0	52.92	0.0	−0.48031
2			−0.28567	53.34	−5.893	0.0	4.754	0.0	2.563
	848	499.0	−2.48280	249.2	66.09	0.0	−5.011	0.0	−1.231
	1000	0.0	−6.39740	695.4	0.667	0.0	−0.837	0.0	−0.1864
	1042	0.0	19.17200	−1775.0	−8.495	0.0	10.43	0.0	2.437
	1060	0.0	−5.53630	332.0	2.930	0.0	−2.236	0.0	−0.4774
	1184	899.6	0.23819	8.416	−0.07295	0.0	0.1005	0.0	0.01786
	1665	836.8	0.52121	3.284	0.0480	0.0	84.26	0.0	−3.329
3		1.09570		1.852	2.963	0.0	−1.862	0.0	−2.01
4			1.66572	0.0	−0.224	0.0	−4.3628	−98.76	0.0
5		0.18343		56.67	0.2384	0.0	0.01747	0.0	0.003869
	848	391.0	−0.02828	2.451	31.14	0.0	0.1861	0.0	0.03834
	1300	0.0	0.86812	15.82	19.74	0.0	889.6	0.0	−14.48
6			0.39874	46.44	−1.642	0.0	1.402	0.0	0.3575
	956	335.0	−0.69915	72.45	78.24	0.0	−0.07284	0.0	−0.01758
	1250	0.0	1.97400	43.23	61.97	0.0	2404.0	0.0	−43.270
7			0.68435	1.194	1.697	0.0	1.348	0.0	−1.188
8		0.39874		46.44	−1.642	0.0	1.402	0.0	0.3575
	848	499.0	−0.69915	72.45	78.24	0.0	−0.07284	0.0	−0.01758
	1000	0.0	1.97400	43.23	61.97	0.0	2404.0	0.0	−43.270
9			0.13305	75.826	−1.3588	0.0	0.60498	0.0	0.80394
	598	398.0	0.71653	−10.605	3.9706	0.0	11.782	0.0	−1.4193
	1000	0.0	−2.28370	147.15	450.57	0.0	−2500.9	0.0	−6.8808
10			0.72148	0.0017918	−20.421	3.4213	1.2495	−0.37844	0.27782
11			1.42680	0.0015857	2.3997	−0.83168	−55.659	0.019122	0.026224

* Sources for standard enthalpy $\Delta H^0_{f,1,298}$ (denoted as H), entropy $S^0_{1,298}$ (denoted as S), molar volume $V^0_{1,298}$ (denoted as V), thermal capacity $C_P(T)$ (denoted as Cp) of solid phases: 1 = H, S, and V, Robie et al. (1978); Cp, Robie et al. (1978) and Chatterjee (1989). 2 = H and S, Robie et al. (1978); Cp, Barin and Knacke (1978); V, Mao et al. (1967). 3 = H, S, and Cp, Robie et al. (1982); V, Akimoto et al. (1976). 4 = H and S, Saxena et al. (1986); Cp, Fei and Saxena (1986); V, Syono et al. (1971). 5 = H and S, assessed in this study; Cp, Haas (1988); V, Mao et al. (1974). 6 = H and S, assessed in this study; Cp, Haas (1988); V, Liebermann and Schreiber (1968). 7, 8 = H, S, V, Fei and Saxena (1986); Cp, Chatterjee (1989). 9 = H, assessed in this study; S, JANAF (1985): Cp, this study (based on data in JANAF, 1985); V, Robie et al. (1982). 10 = H, S, and V, Robie et al. (1978); Cp, this study (based on data in JANAF, 1985). 11 = H, S, and V, Weast et al. (1988); Cp, this study (based on data in Weast et al., 1988).

** The real $C_P(T)$ coefficients equal the listed values multiplied by the relative factors. For example, $a = 1.01490 \times 10^2$ for quartz. T in K.

(1973), and Hemingway (1990). H_2O is always included in the system (HMW), and then the f_{H_2} is also a useful indicator of redox condition for the system. Figure 1 shows the calculated log f_{O_2} in the HM buffer at various T and 2 kbar conditions compared with experimental data from Eugster and Wones (1962), Chou (1978), and Myers and Eugster (1983). The pressure dependence of log f_{O_2} and log f_{H_2} for the assemblage HMW is as follows: log f_{O_2} changes about +0.15 at 1 kbar or +1.5 at 10 kbar; log f_{H_2} changes rapidly at low pressure, with a smaller increase at higher pressure (Fig. 2a). The theoretical curves compare well with the experimental results. Magnetite and hematite, if replaced by pyrite or pyrrhotite in the system Fe-O-H-S, result in the assemblage HMPyW or MPyW/MPoW (low f_{O_2} and high f_{S_2}) or HPyW (high f_{O_2} and high f_{S_2}).

Fay + Qtz + Mt f_{O_2} buffer

The FQM (fayalite + quartz + magnetite) equilibrium has been determined experimentally by Eugster (1957), Wones and Gilbert (1969), Hewitt (1978), Chou (1978), Myers and Eugster (1983), and Kishima and Sakai (1984) and calculated thermodynamically by Eugster and Wones (1962), Taylor and Schmalzried (1964), and Frantz and Eugster (1973). Most experiments and thermochemical calculations are for the Fe-Si-O-H system. Figure 1 shows the calculated isobaric log f_{O_2}-T curve of the FQM buffer at 2 kbar. The pressure dependence of f_{O_2} for this buffer

TABLE 2. Summary of univariant and invariant buffering reactions and divariant nonbuffering reactions in the Fe-Si-O-H-S system

No.	Name*	Abbreviation: Pure**	Abbreviation: With H_2O†	Reaction
	Univariant buffering reactions			
1	Hm + Mt f_{O_2} buffer	HM	HMW	$4Fe_3O_4 + O_2 = 6Fe_2O_3$
2	Fay + Qtz + Mt f_{O_2} buffer	FQM	FQMW	$3Fe_2SiO_4 + O_2 = 3SiO_2 + 2Fe_3O_4$
3	Fay + Qtz + Fe f_{O_2} buffer	FQI	FQIW	$2Fe + SiO_2 + O_2 = Fe_2SiO_4$
4	Fay + Qtz + Wüs f_{O_2} buffer	FQW	FQWW	$Fe_2SiO_4 + xO_2 = SiO_2 + 2FeO_{1+x}$
5	Mt + Fe f_{O_2} buffer	MI	MIW	$3Fe + 2O_2 = Fe_3O_4$
6	Wüs + Fe f_{O_2} buffer	WI	WIW	$2Fe + (1 + x)O_2 = 2FeO_{1+x}$
7	Wüs + Mt f_{O_2} buffer	WM	WMW	$6FeO_{1+x} + (1 - 3x)O_2 = 2Fe_3O_4$
8	Po + Py f_{S_2} buffer	PP	PPW	$2Fe_{1-x}S + (1 - 2x)S_2 = 2(1 - x)\ FeS_2$
9	Fe + Po f_{S_2} buffer	IP	IPW	$2(1 - x)Fe + S_2 = 2Fe_{1-x}S$
	Invariant buffering reactions			
1	Po + Py + Mt f_{O_2}-f_{S_2} buffer	PPM	PPMW	$6Fe_{1-x}S + 3FeS_2 + (6 - 4x)O_2 = (3 - 2x)Fe_3O_4 + 6S_2$
2	Hm + Mt + Py f_{O_2}-f_{S_2} buffer	HMPy	HMPyW	$7FeS_2 + 5O_2 = 2Fe_2O_3 + Fe_3O_4 + 7S_2$
3	Fay + Qtz + Mt + Po f_{O_2}-f_{S_2} buffer	FQMPo	FQMPoW	$3Fe_2SiO_4 + 6Fe_{1-x}S + (5 - 4x)O_2 = 3SiO_2 + 2(2 - x)Fe_3O_4 + 3S_2$
4	Fay + Qtz + Fe + Po f_{O_2}-f_{S_2} buffer	FQIPo	FQIPoW	$2xFe + 2Fe_{1-x}S + SiO_2 + O_2 = Fe_2SiO_4 + S_2$
5	Fay + Qtz + Wüs + Po f_{O_2} buffer	FQWPo	FQWPoW	$Fe_2SiO_4 + 2Fe_{1-x}S + (1 + x - x^2)O_2 = SiO_2 + 2(2 - x)FeO_{1+x} + S_2$
6	Mt + Fe + Po f_{O_2}-f_{S_2} buffer	MIPo	MIPoW	$(1 - 2x)Fe + 2Fe_{1-x}S + 2O_2 = Fe_3O_4 + S_2$
7	Wüs + Fe + Po f_{O_2}-f_{S_2} buffer	WIPo	WIPoW	$2xFe + 2Fe_{1-x}S + (1 + x)O_2 = 2Fe_{1+x}O + S_2$
8	Wüs + Mt + Po f_{O_2}-f_{S_2} buffer	WMPo	WMPoW	$6Fe_{1-x}S + 6FeO_{1+x} + (5 - 7x)O_2 = 2(2 - x)Fe_3O_4 + 3S_2$
9	Hm + Py + $FeSO_4$ f_{O_2}-f_{S_2} buffer	HPyFS	HPyFSW	$2FeS_2 + 2Fe_2O_3 + 9O_2 + S_2 = 6FeSO_4$
10	Mt + Py + $FeSO_4$ f_{O_2}-f_{S_2} buffer	MPyFS	MPyFSW	$FeS_2 + Fe_3O_4 + 6O_2 + S_2 = 4FeSO_4$
	Divariant nonbuffering reactions			
1	Mt + Po	MPo	MPoW	$6Fe_{1-x}S + 4O_2 = 2(1 - x)Fe_3O_4 + 3S_2$
2	Mt + Py	MPy	MPyW	$3FeS_2 + 2O_2 = Fe_3O_4 + 3S_2$
3	Hm + Py	HPy	HPyW	$4FeS_2 + 3O_2 = 2Fe_2O_3 + 4S_2$
4	Fay + Qtz + Po	FQPo	FQPoW	$2FeS + SiO_2 + O_2 = Fe_2SiO_4 + S_2$
5	Wüs + Po	WPo	WPoW	$2Fe_{1-x}S + (1 - x)(1 + x)O_2 = 2(1 - x)FeO_{1+x} + S_2$
6	Hm + $FeSO_4$	HFS	HFSW	$2Fe_2O_3 + 5O_2 + 2S_2 = 4FeSO_4$
7	Mt + $FeSO_4$	MFS	MFSW	$2Fe_3O_4 + 8O_2 + 3S_2 = 6FeSO_4$
8	Py + $FeSO_4$	PyFS	PyFSW	$2FeS_2 + 4O_2 = 2FeSO_4 + S_2$

* Mineral abbreviations same as in Table 1.
** Pure buffers without H_2O.
† Buffer-H_2O equilibrium assemblages.

is not significant (Eugster and Wones, 1962; Chou, 1978; Myers and Eugster, 1983); the variation of log f_{O_2} from 1 bar to 5 kbar is ±0.09 at 300 °C and ±0.002 at 1200 °C. Figure 2b shows the isobaric lines of log f_{H_2} (P = 0.001–5 kbar) of the assemblage FQMW, which are consistent with previous experimental and thermodynamic studies.

Since the fayalite + quartz assemblage is less stable than fayalite + ferrosilite at high pressures, FQM is replaced by the fayalite + ferrosilite + magnetite f_{O_2} buffer $6Fe_2SiO_4 + O_2 = 3Fe_2Si_2O_6 + 2Fe_3O_4$ because of the replacement reaction $Fe_2SiO_4 + SiO_2 = Fe_2Si_2O_6$. Furthermore, FQM is less stable than wüstite + magnetite + quartz at higher temperatures; for instance, at a pressure of 2 kbar, FQM is replaced by WM buffer with quartz at temperatures higher than 1900 °C, with f_{O_2}, f_{H_2}, and f_{H_2O} as 1.37×10^{-4}, 125, and 1875 bars, respectively. Note that quartz would melt at temperatures lower than 1811 K depending on the fluid medium. If S is present in the system (e.g., Fe-Si-O-H-S), magnetite will coexist with or be replaced by pyrrhotite, resulting in the appearance of a very common assemblage (FQMPW) in nature.

Fay + Qtz + Fe f_{O_2} buffer

The FQI (fayalite + quartz + Fe) equilibrium has been determined experimentally by Darken (1948) and Myers and Eugster (1983) and calculated thermodynamically by Eugster and Wones (1962). Calculated f_{O_2} values at dif-

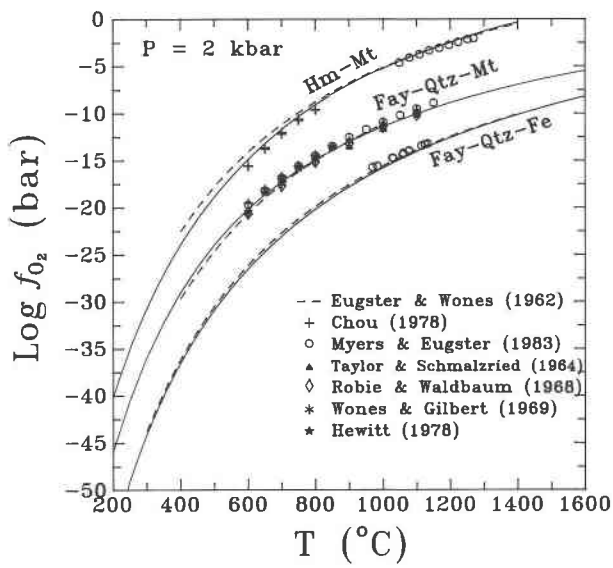

Fig. 1. Log f_{O_2}-T-P relations for the Hm + Mt, Fay + Qtz + Mt, and Fay + Qtz + Fe f_{O_2} buffers at 2 kbar. The theoretical curves are compared with the experimental and calculated data from Eugster and Wones (1962), Chou (1978), and Myers and Eugster (1983) for the Hm + Mt buffer; Eugster and Wones (1962), Taylor and Schmalzried (1964), Robie and Waldbaum (1968), Wones and Gilbert (1969), Hewitt (1978), Chou (1978), and Myers and Eugster (1983) for the Fay + Qtz + Mt buffer; Eugster and Wones (1962) and Myers and Eugster (1983) for the Fay + Qtz + Fe buffer.

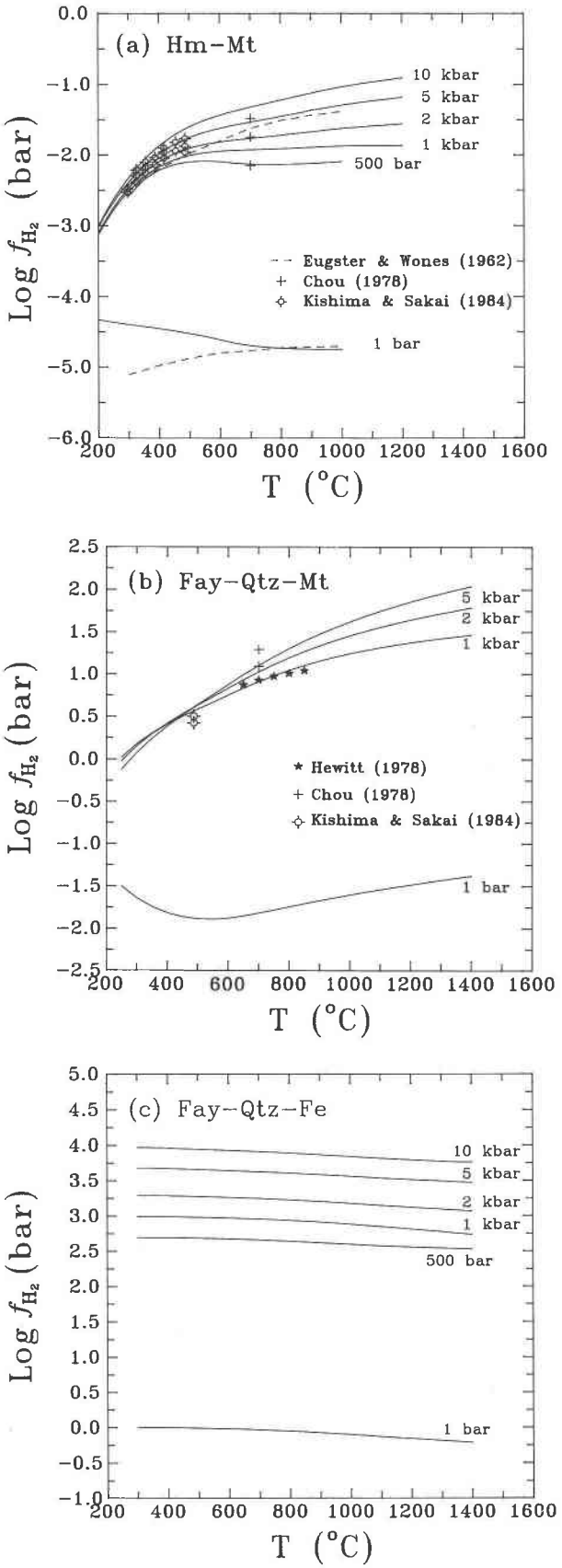

ferent T and 2 kbar for the buffer system are plotted in Figure 1 and show a good fit with the data from previous thermodynamic (Eugster and Wones, 1962) and experimental (Myers and Eugster, 1983) studies. The f_{H_2} (Fig. 2c) is more pressure sensitive than f_{O_2} (Fig. 1). The f_{H_2} of the assemblage FQIW decreases with increasing temperature at all pressures, and it increases with increasing pressure at all temperatures. FQI is less stable than wüstite + Fe + quartz at higher temperatures; for instance, at a pressure of 2 kbar, FQI is displaced by WI buffer with quartz at temperatures higher than 1900 °C.

Mt + Fe, Wüs + Fe, and Wüs + Mt f_{O_2} buffers

In the Fe-O system at low oxidation, there exist three f_{O_2}-buffering equilibria: MI (magnetite + Fe), WI (wüstite + Fe), and WM (wüstite + magnetite). The composition of wüstite is FeO_{1+x}, with x varying from 0 to 0.5. At pressures under 2 kbar and temperatures under 1400 °C, x is less than 0.2. The value of x increases with increasing temperature (Myers and Eugster, 1983). Wüstite has a narrow stability field in log f_{O_2}-T diagram; the stability increases with increasing x value. The buffers, MI, WI, and WM have been studied experimentally by Chipman and Marshall (1940), Darken and Gurry (1945), Norton (1955), Kleman (1965), Swaroop and Wagner (1967), Rizzo et al. (1969), Williams (1971), and Myers and Eugster (1983).

Wüstite in equilibrium with Fe has a relatively fixed composition of $x = 0.05$, without obvious variation due to temperature (Rizzo et al., 1969). In contrast, x increases with f_{O_2} and temperature when wüstite is in equilibrium with magnetite.

The f_{O_2} and f_{H_2} of the MIW, WIW, and WMW buffering assemblages are calculated for systems in which wüstite composition ranges from FeO to $FeO_{1.2}$. The logf_{O_2} values at 2 kbar and various temperatures are plotted in Figure 3a. The low temperature limits and the fluid proportion for the stability field of wüstite are listed in Table 3. Wüstite will not be stable above 585, 576, 567, 506, and 335 °C at 1 bar, 1 kbar, 2 kbar, 10 kbar, and 40 kbar, respectively; These results are comparable to experimental data (Darken and Gurry, 1945).

Figure 3a also shows the comparison of the calculated result of f_{O_2} at a pressure of 2 kbar with previous studies. Note that because wüstite changes composition with temperature, the fit is very good. For stoichiometric FeO, there is a large discrepancy between the theoretical curve and experimental data (see the dashed line in Fig. 3a). Figure 3b shows that f_{H_2} is much more sensitive to pres-

←

Fig. 2. Log f_{H_2}-T-P relations for the (**a**) Hm + Mt + H_2O, (**b**) Fay + Qtz + Mt + H_2O, and (**c**) Fay + Qtz + Fe + H_2O buffering assemblages at various pressures. The experimental and calculated data from Eugster and Wones (1962), Chou (1978), and Kishima and Sakai (1984) for Hm + Mt + H_2O, and Kishima and Sakai (1984), Chou (1978), and Hewitt (1978) for Fay + Qtz + Mt + H_2O are plotted for comparison.

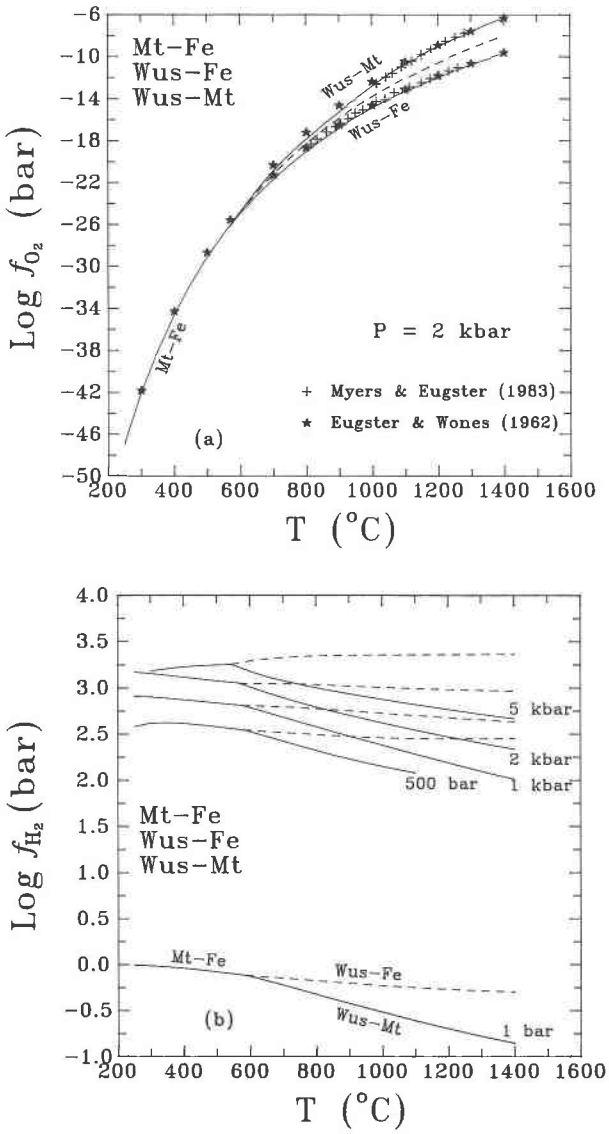

Fig. 3. Log f_{O_2}-log f_{H_2}-T-P relations of the Mt + Fe/Wüs + Fe/Wüs + Mt buffering system. (**a**) Log f_{O_2}-T relation of the Mt + Fe, Wüs + Fe, and Wüs + Mt f_{O_2} buffers at 2 kbar. The experimental data from Myers and Eugster (1983) and calculated data from Eugster and Wones (1962) are plotted for comparison. The dashed line corresponds to wüstite of stoichiometric FeO. (**b**) Log f_{H_2}-T relation of the Mt + Fe + H_2O, Wüs + Fe + H_2O, and Wüs + Mt + H_2O assemblages at various pressures.

sure than f_{O_2}. The f_{H_2} values of the assemblage MIW decrease with increasing temperatures and decreasing pressures. However, f_{H_2} for MIW or WIW increases with temperature above 5 kbar.

Po + Py f_{S_2} buffer

There are several previous thermodynamic and experimental studies of the pyrite + pyrrhotite f_{S_2} buffer (Toulmin and Barton, 1964; Giletti et al., 1968; Schneeberg, 1973; Craig and Scott, 1974; Rau, 1976; Hutcheon, 1978; Gamble, 1978, 1982; Kissin and Scott, 1982; Powell, 1983; Barker and Parks, 1986). For the PP (pyrite + pyrrhotite) f_{S_2}-buffering equilibrium, the log f_{S_2}-T-P relation depends on the composition of pyrrhotite, i.e., $Fe_{1-x}S$. However, the relationship among composition, temperature, and pressure is complicated (see Arnold, 1958, 1962; Toulmin and Barton, 1964).

TABLE 3. *P-T* path and log f_{O_2}-log f_{H_2} conditions of invariant reaction point Mt-Wüs-Fe

P(kbar)	T(°C)	log f_{O_2}	log f_{H_2}
0.001	584.95	−25.378	−0.122
0.5	580.24	−25.592	2.540
1	575.66	−25.801	2.807
2	567.11	−26.204	3.048
5	542.92	−27.402	3.255
10	506.13	−29.300	3.285
20	441.85	−33.053	3.102
30	385.85	−36.943	2.901
40	335.40	−41.092	2.812

$Fe_{0.877}S$ was chosen as the composition for which the thermodynamic properties were assessed in this study. We also considered the solid solution in FeS-□S (□ = vacancy) system of varying composition from N_{FeS} = 1.000–0.9000 (i.e., FeS to $Fe_{0.818}S$).

Table 4 shows the log f_{S_2}-T-P relation for the pyrite + pyrrhotite ($Fe_{0.877}S$) equilibrium. The calculated curves compare favorably with previous experimental data (Fig. 4). The decomposition temperature of pyrite, melting incongruently to pyrrhotite ($Fe_{0.877}S$), is 745 °C at 1 bar; it lies a little above the experimental pyrite-pyrrhotite solvus (Arnold, 1962; Toulmin and Barton, 1964; Scott, 1973). If pyrrhotite with different N_{FeS} compositions is considered, the pyrite-pyrrhotite solvus can be approached. At a total pressure of 1 bar, the decomposition temperature is 743 °C and the highest f_{S_2} value of pyrite-pyrrhotite solvus is about 0.8 bars.

The pyrite-pyrrhotite solvus changes rapidly with increasing pressure (see Table 4). In fact, the experimental investigations of pyrite-pyrrhotite solvi were performed in systems that were saturated with S_2 (Arnold, 1958, 1962; Kullerud and Yoder, 1959). Kullerud and Yoder (1959) reported the internal pressure of the system to be about 10–25 bars at 743 °C. Accordingly, the highest f_{S_2} value of pyrite-pyrrhotite solvus reported by them is actually 2.85 bars (corresponding to the decomposition temperature 747 °C on the calculated 20-bar curve in the case of varied pyrrhotite composition), which is a little higher than that at 1 bar. The pressure dependence of f_{S_2} also should be emphasized; the value of f_{S_2} at a given temperature decreases with increasing pressure, especially at high pressures. This is a reverse conclusion to that of Toulmin and Barton (1964). The problem is that in the studies of Toulmin and Barton (1964) the pressure dependence of the activity coefficient of S_2 and of volumes of pyrite and pyrrhotite in the calculation were not considered.

If there is relatively high f_{O_2} in the system, magnetite

TABLE 4. Log f_{S_2}-T-P relations of Po + Py f_{S_2} buffer

	P (bar)						
T (°C)	1	500	1000	2000	4000	5000	10000
200.0	−15.177	−15.189	−15.207	−15.307	−15.537	−15.654	−16.183
250.0	−12.380	−12.401	−12.425	−12.519	−12.730	−12.838	−13.319
300.0	−10.064	−10.090	−10.117	−10.206	−10.402	−10.501	−10.943
350.0	−8.110	−8.139	−8.168	−8.252	−8.434	−8.526	−8.934
400.0	−6.444	−6.475	−6.505	−6.584	−6.754	−6.840	−7.220
450.0	−5.012	−5.044	−5.074	−5.149	−5.309	−5.389	−5.744
500.0	−3.771	−3.802	−3.833	−3.903	−4.054	−4.130	−4.462
550.0	−2.685	−2.717	−2.747	−2.814	−2.956	−3.027	−3.341
600.0	−1.729	−1.717	−1.790	−1.853	−1.988	−2.056	−2.352
650.0	−0.883	−0.913	−0.942	−1.003	−1.131	−1.195	−1.473
700.0	−0.128	−0.153	−0.186	−0.244	−0.366	−0.427	−0.693
750.0	—	0.518	0.490	0.435	0.318	0.260	0.008
800.0		1.125	1.098	1.045	0.934	0.878	0.638
850.0		1.674	1.648	1.596	1.490	1.437	1.208
900.0		2.172	2.146	2.097	1.995	1.944	1.725
950.0		—	2.601	2.553	2.455	2.406	2.194
1000.0			—	2.971	2.876	2.829	2.630
1050.0				—	3.263	3.218	3.027
1100.0					—	3.576	3.393
1150.0						—	3.731
1200.0							—

coexists with pyrrhotite and pyrite, resulting in PPM equilibrium.

Po + Py + Mt f_{O_2}-f_{S_2} buffer

The PPM (pyrite + pyrrhotite + magnetite) equilibrium controls f_{S_2} and f_{O_2} in Fe-O-H-S system through the univariant S-buffering reaction PP and two divariant reactions MPo and MPy. This buffer has been used in hydrothermal experiments by Raymahashay and Holland (1968), Crerar et al. (1978), Spry and Scott (1986), Janecky et al. (1986), and Wood et al. (1987). Recently,

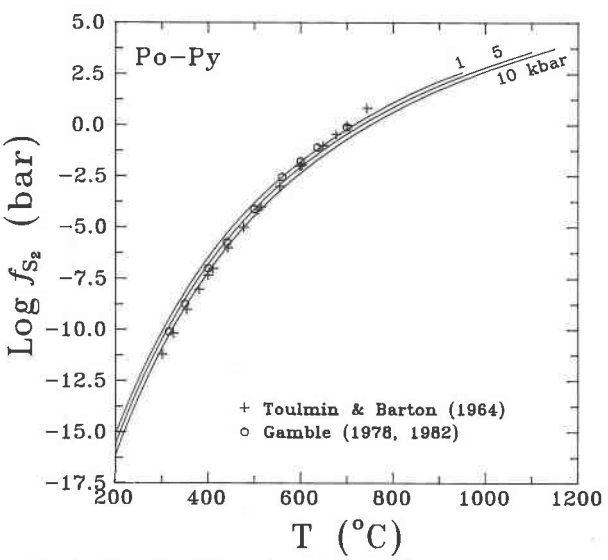

Fig. 4. Log f_{S_2}-T-P relation of Po-Py f_{S_2} buffer. The isobaric log f_{S_2}-T curves are plotted for 1, 5, and 10 kbar. The theoretical curves are compared with experimental data from Toulmin and Barton (1964), Gamble (1978, 1982).

Kishima (1989) measured the equilibrium concentrations of fluid components at pressures from 100 bars to 1 kbar and used their data to explain some geochemical problems related to the volcanic rock-H_2O interaction systems (Haggerty, 1976; D'Amore and Panichi, 1980; Arnórsson, 1985) and the diagenetic origin of H_2S-rich fluid inclusions (Roedder, 1971; Mironova et al., 1973; Bény et al., 1982; Guilhaumou et al., 1984). As mentioned in their work, the pressure dependence of the log f_{O_2} at high pressures is larger than that at low pressures (<1 kbar).

Log f_{S_2} of the system is the same as that of the PP buffer. Log f_{O_2}, log f_{H_2}, log f_{SO_2}, log f_{H_2O}, and log f_{H_2S} of the assemblage PPMW are shown in Table 5 and Figures 5a and 5b. With increasing temperature, there is no obvious change in log f_{O_2}, but log f_{H_2} increases slightly and log f_{H_2S} and log f_{SO_2} increase rapidly. Log f_{O_2} has a tendency to decrease slightly with increasing pressure, which is the opposite of the results of Kishima (1989). The f_{H_2O}, f_{H_2S}, and f_{H_2} increase with increasing pressure, but the f_{SO_2} decreases. The calculated f_{O_2}, f_{H_2}, and f_{H_2S} of the assemblage PPMW are compared with Kishima's experimental data in Figures 5a and 5b. The calculated log f_{O_2} and log f_{H_2S} are higher than the measured ones, whereas the calculated f_{H_2} is lower.

At high temperature, the assemblage PPMW is replaced by the divariant assemblage MPoW. As the breakdown temperature is approached, SO_2 becomes the dominant species, whereas f_{H_2}, f_{H_2O}, and f_{H_2S} decrease swiftly (see Fig. 5b). Pyrite is converted to magnetite. At a pressure of 2 kbar, for instance, the PPMW assemblage is unstable at temperatures higher than 745 °C, with log f_{SO_2} equal to 3.3006. Table 5 also lists the breakdown temperatures and log f_{O_2}, log f_{S_2}, and log f_{SO_2} values for the assemblage PPMW at 1, 2, and 5 kbar. The breakdown temperature for this assemblage increases with pressure

TABLE 5. Log f_{O_2}-T-P relations of Po + Py + Mt f_{O_2}-f_{S_2} buffer

	P (bar)		
T (°C)	1000	2000	5000
200.0	−41.725	−41.955	−42.657
300.0	−31.940	−32.133	−32.718
400.0	−25.020	−25.185	−25.682
500.0	−19.910	−20.054	−20.486
600.0	−16.009	−16.137	−16.517
700.0	−12.948	−13.062	−13.401
800.0	—	—	−10.891
900.0			—

P (kbar)	T (°C)	log f_{O_2}	log f_{S_2}	log f_{SO_2}
1	714.24	−12.565	0.014	2.999
2	745.11	−11.881	0.371	3.301
5	806.84	−10.737	0.958	3.698

and is always lower than the decomposition temperature of pyrite (on pyrite-pyrrhotite solvus) (see Table 4); therefore pyrite will not melt incongruently to pyrrhotite.

As shown in Figure 5, (1) the f_{O_2} of the PPMW buffering assemblage is between the HMW and FQMW buffering assemblages; (2) H_2S is the dominant S-bearing species in the fluid phase at low temperatures, whereas SO_2 is the most abundant S-bearing species as temperature increases toward the breakdown point; (3) the f_{H_2} is always lower than f_{H_2S}; (4) as the breakdown temperature is approached, f_{H_2}, f_{H_2O}, and f_{H_2S} drop rapidly to the minimum values.

At a given temperature, magnetite converts to pyrite at lower f_{O_2}, resulting in univariant equilibrium assemblage PPW; pyrrhotite will disappear at higher f_{S_2} and higher f_{O_2}, resulting in pyrite in equilibrium with magnetite (MPyW); pyrite will disappear at low f_{S_2} and lower f_{O_2}, and the assemblage of pyrrhotite and magnetite (MPoW) will form (Eriksson and Fredriksson, 1983). The MPo, MPy divariant equilibria are functions of both f_{O_2} and f_{S_2}. Inside the stability field of the MPoW nonbuffering assemblage at a certain temperature and pressure, the f_{O_2} and f_{S_2} values might be fixed empirically and graphically below the upmost stability values (discussed later), based on the recommended stability log f_{S_2}-N^{Po}_{FeS}-T relations (Toulmin and Barton, 1964; Whitney, 1984). However, the internal equilibrium in fluid in equilibrium with pyrrhotite + magnetite assemblage should be considered at all times; otherwise, it is easy to make mistakes, such as $P_{fluid} > P_{system}$. This study specifies the upper limits of f_{O_2}, f_{S_2}, and f_{SO_2} for MPoW and MPyW assemblages at different temperatures and a pressure of 2 kbar, using the technique of free energy minimization instead of any empirical or graphic estimation. The results show that the calculated upper limit for MPoW assemblage is much lower than estimated by Whitney (1984) (see below).

Hm + Mt + Py f_{O_2}-f_{S_2} buffer

The HMPy (hematite + magnetite + pyrite) equilibrium is controlled by the univariant O-buffering reaction HM and two divariant reactions MPy and HPy. The assemblage HMPyW is stable under high f_{O_2} and high f_{S_2}. The f_{O_2} value of the HMPy buffer is the same as that of the HM buffer. The f_{S_2} values calculated at various temperatures and pressures are shown in Figure 6. Like the PP buffer, the f_{S_2} values for the HMPy buffer increase with increasing temperature and decreasing pressure (Table 6, Fig. 6). Although the pressure dependence is much smaller than the temperature dependence, it is still sig-

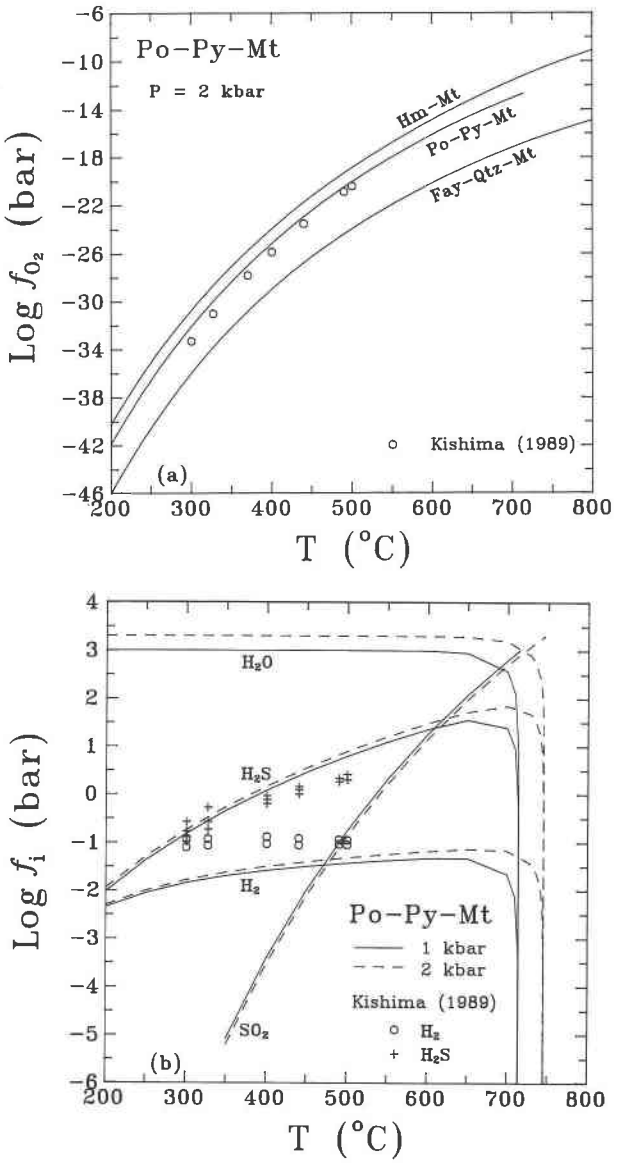

Fig. 5. Log f_i-T-P relations of the Po + Py + Mt + H_2O f_{O_2}-f_{S_2} buffering system. (**a**) Log f_{O_2}-T relation of the Po + Py + Mt f_{O_2}-f_{S_2} buffer at 2 kbar. The experimental data from Kishima (1989) are plotted for comparison. The diagram also shows Hm + Mt and FQM buffers, which jointly limit the Po + Py + Mt buffer. (**b**) Log f_i-T-P relations of the Po + Py + Mt + H_2O assemblage at 1 and 2 kbar. The fluid fugacities of H_2O, H_2S, H_2, and SO_2 can be compared with the experimental data of Kishima (1989). See discussion in the text.

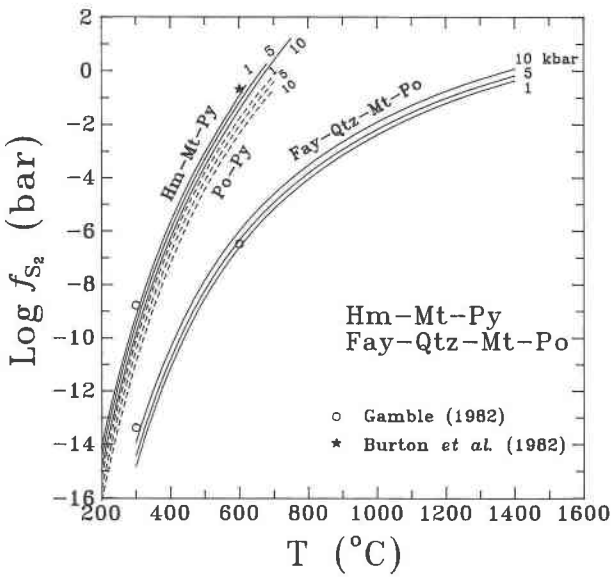

Fig. 6. Log f_{S_2}-T relations of the Hm + Mt + Py and Fay + Qtz + Mt + Po f_{O_2}-f_{S_2} buffers at 1, 5, and 10 kbar. The theoretical curves are compared with experimental data from Gamble (1982), Burton et al. (1982) for Hm + Mt + Py, and Gamble (1982) for Fay + Qtz + Mt + Po. The Po + Py f_{S_2} buffer curves at 1, 5, and 10 kbar are also plotted in dashed lines.

nificant. Figure 6 also shows that the log f_{S_2}-T curve of the HMPy buffer will never cross the same curve for the PP buffer at any temperature and pressure, implying pyrrhotite is never in equilibrium with coexisting hematite and magnetite. Similarly, at high temperature it is replaced by the divariant assemblage HPyW because the fluid can be no longer in equilibrium with magnetite. This happens when SO_2 becomes the dominant species, whereas f_{H_2}, f_{H_2O}, and f_{H_2S} decrease. At a pressure of 2 kbar, the HMPyW assemblage is unstable at temperatures higher than 623.9 °C and with log f_{SO_2} equal to 3.3010. The breakdown temperatures and log f_{O_2}, log f_{S_2}, and log f_{SO_2} values for the HMPyW buffering assemblage at different pressures are also listed in Table 6. The breakdown temperature for this assemblage also increases with pressure but is always much lower than that for the PPMW assemblage (see Table 6).

Figure 7a and Table 6 show the temperature-pressure relations for f_{H_2S}, f_{SO_2}, f_{H_2}, and f_{H_2O} in the HMPyW assemblage. One can conclude that (1) H_2S is the dominant S-bearing species in the fluid phase at low temperatures and SO_2 is the most abundant S-bearing species at high temperatures, with the latter being very significant as the breakdown temperature is approached; (2) f_{H_2O} and f_{H_2} increase with increasing pressure, but f_{SO_2} decreases rapidly; (3) f_{H_2S} reaches a maximum at pressure of about 5

Table 6. Log f_{S_2}-T-P relations of Hm + Mt + Py and Fay + Qtz + Mt + Po f_{O_2}-f_{S_2} buffers

		Hm + Mt + Py buffer		
P (kbar)	T (°C)	log f_{O_2}	log f_{S_2}	log f_{SO_2}
0.001	482.35	−19.437	−3.435	−0.0002
1	603.75	−14.619	−0.881	3.000
2	623.89	−14.029	−0.562	3.301
4	651.97	−13.318	−0.183	3.602
5	663.97	−13.043	−0.038	3.699
10	719.51	−11.836	0.590	4.000

	P (bar)					
T (°C)	1	1000	2000	4000	5000	10000
200.0	−14.143	−14.149	−14.226	−14.408	−14.501	−14.911
250.0	−11.431	−11.455	−11.529	−11.699	−11.786	−12.164
300.0	−9.186	−9.222	−9.292	−9.452	−9.533	−9.885
350.0	−7.293	−7.335	−7.403	−7.554	−7.630	−7.959
400.0	−5.669	−5.716	−5.781	−5.924	−5.996	−6.307
450.0	−4.257	−4.307	−4.369	−4.505	−4.574	−4.868
500.0	—	−3.064	−3.124	−3.254	−3.319	−3.600
550.0		−1.957	−2.015	−2.139	−2.201	−2.469
600.0		−0.953	−1.009	−1.128	−1.188	−1.445
650.0		—	—	−0.217	−0.274	−0.521
700.0				—	—	0.298
750.0						—
			Fay + Qtz + Mt + Po buffer			
200.0	−20.472	−20.263	−20.127	−19.886	−19.771	−19.162
300.0	−14.998	−14.852	−14.743	−14.547	−14.453	−13.946
400.0	−11.278	−11.168	−11.076	−10.910	−10.829	−10.391
500.0	−8.630	−8.541	−8.461	−8.315	−8.244	−7.856
600.0	−6.698	−6.622	−6.551	−6.420	−6.355	−6.004
700.0	−5.253	−5.187	−5.123	−5.002	−4.943	−4.619
800.0	−4.117	−4.058	−3.998	−3.886	−3.831	−3.528
900.0	−3.196	−3.142	−3.086	−2.980	−2.928	−2.640
1000.0	−2.434	−2.384	−2.331	−2.229	−2.179	−1.904
1100.0	−1.795	−1.748	−1.697	−1.599	−1.551	−1.284
1200.0	−1.255	−1.210	−1.161	−1.066	−1.020	−0.759
1300.0	−0.801	−0.755	−0.707	−0.615	−0.569	−0.313
1400.0	—	−0.372	−0.325	−0.235	−0.190	0.064

kbar but decreases rapidly at higher pressures; (4) the abundance of all species, except SO_2 and S_2, decreases when HMPy is replaced by HMFS or MPyFS; (5) when the breakdown temperature is approached, f_{H_2}, f_{H_2O}, and f_{H_2S} drop rapidly to the "minimum" values.

At a given temperature, pyrite may be oxidized to hematite (HMW) at lower f_{S_2} and fixed f_{O_2}; hematite may be replaced by pyrite (MPyW) at lower f_{O_2} and lower f_{S_2}; magnetite may be displaced by hematite and pyrite (HPyW) at higher f_{O_2} and higher f_{S_2}. This study also specifies the upper limits of f_{O_2}, f_{S_2}, and f_{SO_2} for MPyW and HPyW nonbuffering assemblages at different temperatures and a pressure of 2 kbar (see below).

Fay + Qtz + Mt + Po f_{O_2}-f_{S_2} buffer

The FQMPo (fayalite + quartz + magnetite + pyrrhotite) equilibrium is a combination of the f_{O_2}-f_{S_2} buffer of the univariant reaction FQM and the two divariant reactions MPo and FQPo. The terminal oxidation-sulfidation reactions in the f_{O_2}-f_{S_2} space of fayalite (Fay → Mt or Fay → Po) are specified by this invariant reaction point. The calculated log f_{S_2} values at various temperatures and pressures are shown in Figure 6 and Table 6. At 1 bar, pyrrhotite will not be stable at 1200 °C and above. The data at 1, 5, and 10 kbar are shown in Figure 6 for comparison with the PP f_{S_2} buffer. The f_{S_2} value for the FQMPo buffer increases with temperature and pressure, which is the opposite pressure trend of the PP f_{S_2} buffer.

Figure 7b illustrates the temperature-pressure relations for f_{H_2S}, f_{SO_2}, f_{H_2}, and f_{H_2O} in the FQMPW assemblage. We conclude that (1) H_2S is much more abundant than SO_2, second only to H_2O; (2) f_{H_2O} increases with increasing pressure and decreasing temperature; (3) f_{SO_2} increases with temperature and pressure; (4) f_{H_2} and f_{H_2S} increase with pressure at high temperatures but decrease with increasing pressure at low temperatures.

At a given temperature, pyrrhotite may be oxidized to magnetite (FQMW) at lower f_{S_2} and fixed f_{O_2}; magnetite may be replaced by pyrrhotite (FQPoW) at lower f_{O_2} and lower f_{S_2}; fayalite may be displaced by magnetite and pyrrhotite (MPoW) at higher f_{O_2} and higher f_{S_2}. When temperature is higher than the transitional invariant reaction point fayalite-quartz-magnetite-wüstite-pyrrhotite (e.g., 1900 °C at 2 kbar), fayalite converts to wüstite and quartz, so the FQMPoW assemblage is replaced by WMPoW saturated with quartz (at higher f_{O_2} and higher f_{S_2}) or FQWPoW (at lower f_{O_2} and lower f_{S_2}).

Fe + Po f_{S_2} buffer and Fay + Qtz + Fe + Po f_{O_2}-f_{S_2} buffer

At relatively low f_{O_2} and f_{S_2}, metallic Fe may coexist with pyrrhotite, IP (Fe + pyrrhotite equilibrium), as a S buffer that is significant for some natural processes occurring under strong reducing conditions. The IP S-buffering assemblage may be stable with the FQI O-buffering assemblage in the quartz-saturated system, resulting in the FQIPo (fayalite + quartz + Fe + pyrrhotite) equilibrium, which is jointly controlled by the univariant reaction FQI and two divariant reactions MPo and FQPo. Like the FQMPo buffer, this invariant buffering reaction specifies the terminal reduction reaction in the f_{O_2}-f_{S_2} space of fayalite (Fay → Fe).

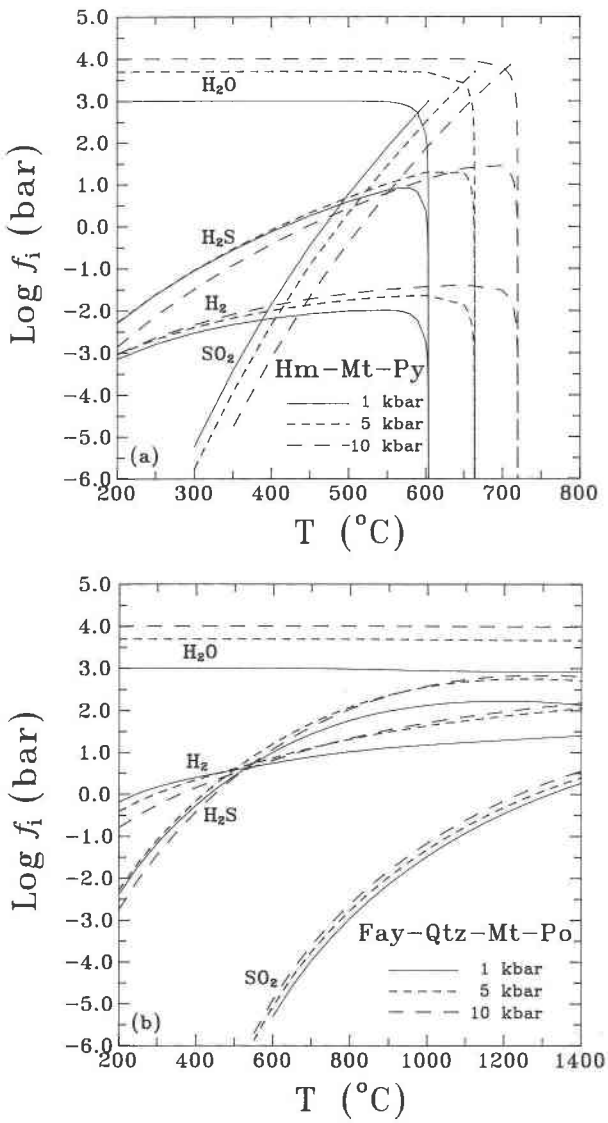

Fig. 7. Log f_i-T-P relations of the (**a**) Hm + Mt + Py + H_2O and (**b**) Fay + Qtz + Mt + Po + H_2O f_{O_2}-f_{S_2} buffering assemblages at 1, 5, and 10 kbar.

The calculated fluid proportions of the IP f_{S_2} buffer and FQIPoW buffering assemblage at different temperatures and a pressure of 2 kbar are listed in Table 7. As temperature increases, f_{H_2} decreases, whereas f_{S_2}, f_{H_2O}, and f_{SO_2} increase, f_{H_2S} has a maximum at a temperature of about 1250 °C.

At a given temperature, pyrrhotite may be oxidized to fayalite (FQIW) at lower f_{S_2} and fixed f_{O_2}; fayalite may be reduced to pyrrhotite and Fe (IPoW saturated with quartz) at lower f_{O_2} and fixed f_{S_2}; Fe may be displaced by fayalite and pyrrhotite (FQPoW) at higher f_{O_2} and higher

TABLE 7. Log f_i-T relations of Fay + Qtz + Fe + Po and Hm + Py + $FeSO_4$ f_{O_2}-f_{S_2} buffers in the Fe-Si-O-H-S system at 2 kbar

T (°C)	log f_{O_2}	log f_{S_2}	log f_{SO_2}	log f_{H_2}	log f_{H_2O}	log f_{H_2S}
			Fay + Qtz + Fe + Po buffer			
200.0	−55.087	−28.029	−31.573	3.293	2.334	−2.713
300.0	−44.199	−21.923	−25.067	3.288	2.342	−1.529
400.0	−36.555	−17.678	−20.460	3.280	2.399	−0.600
500.0	−30.890	−14.546	−17.030	3.269	2.470	0.159
600.0	−26.518	−12.133	−14.373	3.254	2.542	0.777
700.0	−23.032	−10.208	−12.243	3.234	2.611	1.274
800.0	−20.177	−8.628	−10.484	3.208	2.676	1.663
900.0	−17.791	−7.304	−9.004	3.174	2.733	1.956
1000.0	−15.770	−6.186	−7.747	3.135	2.780	2.159
1100.0	−14.043	−5.237	−6.680	3.097	2.817	2.285
1200.0	−12.552	−4.425	−5.766	3.062	2.852	2.345
1300.0	−11.249	−3.726	−4.975	3.034	2.886	2.350
1400.0	−10.102	−3.120	−4.285	3.013	2.921	2.355
			Hm + Py + $FeSO_4$ buffer			
200.0	−33.981	−9.462	−1.184	−6.293	3.301	−3.016
250.0	−29.856	−7.599	−0.216	−5.368	3.301	−2.200
300.0	−26.449	−6.057	0.616	−4.629	3.301	−1.513
350.0	−23.587	−4.762	1.333	−4.025	3.299	−0.917
400.0	−21.150	−3.658	1.954	−3.529	3.292	−0.399
450.0	−19.051	−2.707	2.495	−3.136	3.261	0.035
500.0	−17.224	−1.878	2.970	−2.931	3.103	0.293
539.09	−15.953	−1.302	3.301	—	—	—

f_{S_2}. When temperature is higher than the transitional invariant reaction point fayalite-quartz-Fe-wüstite-pyrrhotite (e.g., 1900 °C at 2 kbar), fayalite changes to wüstite and quartz, so the FQIPoW assemblage is replaced by WIPoW saturated with quartz (at lower f_{O_2}) or FWQPoW (at higher f_{O_2} and higher f_{S_2}).

Mt + Fe + Po/Wüs + Fe + Po/Wüs + Mt + Po buffer

In the absence of quartz, the IP S-buffering assemblage can be in equilibrium with magnetite (MIPo, at low temperature) or wüstite (WIPo, at high temperature) at fixed f_{O_2}-f_{S_2} conditions in the system. The transition of MIPo to WIPo (at lower f_{O_2}) or WMPo (at higher f_{O_2} and higher f_{S_2}) occurs at the temperature of the transitional invariant reaction point magnetite-wüstite-Fe-pyrrhotite (e.g., 567.11 °C at 2 kbar). The f_{S_2} of MIPoW and WIPoW are the same as of the IP f_{S_2} buffer and the FQIPo f_{O_2}-f_{S_2} buffering system (Table 7). If f_{O_2} and f_{S_2} increase at temperatures higher than that of the transitional invariant reaction point magnetite-wüstite-Fe-pyrrhotite, the higher-temperature assemblage WIPoW is displaced by WMPoW.

The calculated fluid proportions of MIPoW/WIPoW/WMPoW f_{O_2}-f_{S_2} buffering assemblages at different tem-

TABLE 8. Log f_i-T relations of Mt + Fe + Po, Wüs + Fe + Po, and Wüs + Mt + Po f_{O_2}-f_{S_2} buffers in the Fe-O-H-S system at 2 kbar

T (°C)	log f_{O_2}	log f_{S_2}	log f_{SO_2}	log f_{H_2}	log f_{H_2O}	log f_{H_2S}	Buffer
200.0	−52.834	−28.029	−29.320	3.123	3.290	−2.883	MIPo
300.0	−42.153	−21.923	−23.021	3.151	3.228	−1.666	
400.0	−34.673	−17.678	−18.578	3.111	3.171	−0.769	
500.0	−29.155	−14.546	−15.295	3.071	3.139	−0.039	
567.11	−26.204	−12.864	−13.541	3.047	3.125	0.375	MIWPo*
600.0	−24.965	−12.133	−12.819	3.047	3.111	0.569	WIPo
700.0	−21.707	−10.208	−10.918	3.040	3.078	1.079	
800.0	−19.045	−8.628	−9.353	3.025	3.059	1.480	
900.0	−16.824	−7.304	−8.037	3.005	3.046	1.786	
1000.0	−14.947	−6.186	−6.924	2.981	3.037	2.005	
1100.0	−13.347	−5.237	−5.984	2.960	3.028	2.148	
1200.0	−11.969	−4.425	−5.184	2.942	3.023	2.225	
1300.0	−10.770	−3.726	−4.496	2.931	3.022	2.246	
1400.0	−9.717	−3.120	−3.900	2.925	3.026	2.217	
600.0	−24.816	−12.002	−12.605	3.005	3.144	0.593	WMPo
700.0	−21.208	−9.770	−10.199	2.887	3.176	1.145	
800.0	−18.294	−7.969	−8.272	2.783	3.192	1.567	
900.0	−15.881	−6.478	−6.681	2.686	3.199	1.881	
1000.0	−13.843	−5.218	−5.336	2.594	3.202	2.102	
1100.0	−12.094	−4.138	−4.182	2.506	3.202	2.244	
1200.0	−10.576	−3.203	−3.179	2.425	3.202	2.319	
1300.0	−9.244	−2.388	−2.301	2.353	3.207	2.338	
1400.0	−8.069	−1.675	−1.530	2.291	3.216	2.306	

* MIWPo is the transitional invariant reaction point (magnetite-Fe-wüstite-pyrrhotite) at which the invariant buffering reaction MIPo converts to WIPo or WMPo.

peratures and a pressure of 2 kbar are listed in Table 8. For three assemblages, the f_{O_2}, f_{S_2}, f_{SO_2}, and f_{H_2S} increase with increasing temperature, whereas f_{H_2} decreases. The f_{H_2O} decreases with temperature in the stability fields of both MIPoW and WIPoW assemblages but increases for the WMPoW assemblage.

Hm + Py + $FeSO_4$ buffer

At relatively high f_{O_2} and f_{S_2}, $FeSO_4$ coexists with pyrrhotite and hematite, formed from three divariant reactions HPy, HFS, and PyFS.

For the f_{O_2}-f_{S_2} buffering assemblage HPyFSW, f_{O_2}, f_{S_2}, f_{SO_2}, f_{H_2}, and f_{H_2S} increase and f_{H_2O} decreases as temperature increases (see Table 7). At temperatures higher than 539.09 °C at a pressure of 2 kbar and a log f_{SO_2} of 3.3010, the assemblage is unstable and f_{H_2}, f_{H_2O}, and f_{H_2S} drop to the minimum values. In this assemblage one solid phase can change to the other two, depending upon f_{O_2}, f_{S_2}, and T. The upper limits of f_{O_2}, f_{S_2}, and f_{SO_2} for PyFSW and HFSW nonbuffering assemblages at different temperatures and a pressure of 2 kbar are affirmed in this study (see below).

Phase equilibria in the Fe-Si-O-H-S system

As an application of the buffers discussed above, we present here some diagrams for phase equilibria in the system at a pressure of 2 kbar. Assemblages that include magnetite, hematite, wüstite, fayalite, pyrite, pyrrhotite, Fe, or quartz occur frequently in magmatic, metamorphic, and hydrothermal systems. Phase equilibria in the Fe-Si-O-H-S system were investigated experimentally and thermodynamically by Barton (1970), Barton and Skinner (1979), Holland (1956a, 1956b), Barton and Toulmin (1964, 1966), Toulmin and Barton (1964), Craig and Scott (1974), Burt (1971, 1972, 1974), Gamble (1978, 1982), Burton (1978), Burton et al. (1982), and Whitney (1984).

Figure 8 shows the phase relations in log f_{O_2}–log f_{S_2} space in the Fe-Si-O-H-S system at 400, 600, and 800 °C. The invariant equilibria MIPo, WIPo, and WMPo and univariant equilibria MI, WI, and WM are impossible in the quartz-saturated Fe-Si-O-H-S system under the temperature-pressure conditions considered in this diagram. However, in the presence of quartz, they are stable when temperature is higher than the transitional

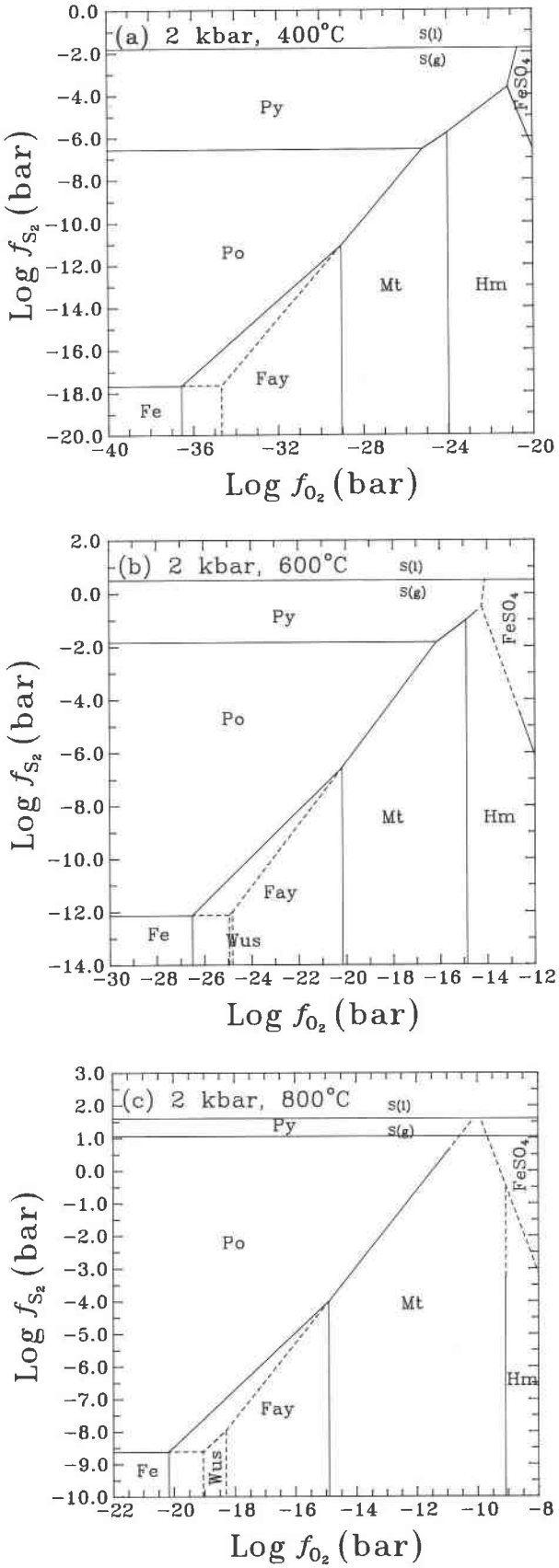

Fig. 8. Log f_{O_2}-log f_{S_2} phase diagrams for the Fe-Si-O-H-S system at 2 kbar. (**a**) 400 °C, (**b**) 600 °C, (**c**) 800 °C. The univariant reaction lines around the invariant reaction points Mt-Fe-Po (**a**), Wüs-Fe-Po (**b**, **c**), and Wüs-Mt-Po (**b**, **c**) in the stability field of fayalite are plotted as dashed lines, implying these univariant and invariant reaction equilibria are impossible in the quartz-saturated Fe-Si-O-H-S system under the temperature-pressure conditions considered. In the upper right area of the diagrams for 600 and 800 °C, the dashed lines indicate that the univariant reactions cannot reach equilibrium because at related T-f_{O_2}-f_{S_2} conditions SO_2 dominates the O-H-S fluid entirely, i.e., $P_{SO_2} \approx P_{system}$.

TABLE 9. The utmost stability log f_i-T relations for pyrite- and pyrrhotite-bearing Fe-O-H-S system at 2 kbar

T (°C)	log f_{O_2}	log f_{S_2}	log f_{SO_2}	Assemblage
200.0	−32.486	−3.482	3.301	PyFS
300.0	−25.554	−2.478	3.301	
400.0	−20.701	−1.862	3.301	
500.0	−17.114	−1.437	3.301	
539.09	−15.953	−1.302	3.301	HPyFS
550.0	−15.683	−1.198	3.301	HPy
600.0	−14.533	−0.756	3.301	
623.89	−14.029	−0.562	3.301	HMPy
650.0	−13.519	−0.340	3.301	MPy
700.0	−12.618	0.051	3.301	
745.11	−11.881	0.371	3.301	PPM
800.0	−10.991	0.570	3.300	MPo
900.0	−9.583	0.887	3.300	
1000.0	−8.394	1.154	3.298	
1100.0	−7.375	1.380	3.296	
1200.0	−6.492	1.573	3.293	
1300.0	−5.717	1.738	3.290	
1400.0	−5.031	1.879	3.285	

invariant reaction point fayalite-quartz-wüstite-magnetite or fayalite-quartz-wüstite-Fe, which is 1900 °C at 2 kbar for both transitional invariant reaction points, implying the invariant reaction FQW is vertical in the log f_i–T space. If there is no SiO_2 in the system, the stability field for fayalite will disappear. At a given temperature, there is an upper limit for f_{O_2}, f_{S_2}, and f_{SO_2} stabilizing some invariant (PPMW, HMPyW, and HPyFSW) and univariant (MPoW, MPyW, HPyW, and PyFSW) assemblages. Such upper limits for f_{O_2}, f_{S_2}, and f_{SO_2} require very low content of H in the bulk fluid composition, and the equilibrium f_{H_2}, f_{H_2O}, and f_{H_2S} values are at the minimum.

Table 9 shows the f_{O_2}-f_{S_2}-f_{SO_2} upper limits of stabilities for some pyrite- or pyrrhotite-bearing assemblages at 2 kbar and various temperatures. At temperatures lower than 539.09 °C, the upper limit is specified by the univariant reaction PyFS. At temperatures between 539.09 and 623.89 °C, it is defined by the univariant reaction HPy. Between 623.89 and 745.11 °C, it is fixed by the univariant reaction MPy. At temperatures higher than 745.11 °C, it is determined by the univariant reaction MPo. Therefore, the Hm + Mt + $FeSO_4$ or Mt + Py + $FeSO_4$ or Hm + Mt + Py + $FeSO_4$ assemblages cannot coexist in equilibrium.

Figure 9 shows the f_{O_2}, f_{S_2}, f_{SO_2}, f_{H_2}, f_{H_2O}, and f_{H_2S} for different invariant reactions at a pressure of 2 kbar and various temperatures. The diagram also illustrates the upper limits of stabilities for the pyrite- and pyrrhotite-bearing assemblages. We conclude the following:

TABLE 10. The stable and unstable assemblages in the Fe-Si-O-H-S system

	Stable assemblages		Unstable assemblages	
Temperature range	Univariant	Invariant	Univariant	Invariant
>PPMW	MPo		MPy HPy PyFS	PPM HMPy HPyFS
HMPyW → PPMW	MPy MPo	PPM	HPy PyFS	HMpy HPyFS
HPyFSW → HMPyW	HPy MPy MPo	HMPy PPM	PyFS	HPyFS
<HPyFSW	PyFS HPy MPy MPo	HPyFS HMPy PPM		

1. At a given temperature, the order in which the stability values of f_{O_2}, f_{S_2}, and f_{SO_2} for all sulfide-bearing invariant reactions increase is the same, i.e., FQIPo < MIPo/WIPo < WMPo < FQMPo < PPM < HMPy < HPyFS, with only one exception that the stability f_{S_2} values for FQIPo and MIPo/WIPo are equal.

2. The f_{H_2} values for FQMPo, FQIPo, and MIPo/WIPo/WMPo assemblages in Fe-Si-O-H-S system are almost the same as those for the pure FQM, FQI, and MI/WI/WM fluid-equilibrated assemblages in the Fe-Si-O-H system. Similarly the f_{H_2} for HMPyW, over much of its stability temperature range, is nearly the same as for pure HMW. This implies the interaction energies among fluid species are small over the temperature-pressure range considered.

3. The order in which the stability values of f_{H_2O} for all sulfide-bearing invariant reactions increase is FQMPo ≈ HPyFS ≈ HMPy ≈ PPM < MIPo/WMPo < WIPo < FQIPo.

4. The order in which the stability values of f_{H_2S} for all sulfide-bearing invariant reactions increase is PPM < HMPy < FQMPo < HPyFS < FQIPo < MIPo/WMPo < WIPo. The stability value for HPyFS crosses those of MIPo and FQIPo at low temperatures.

5. As the breakdown temperatures for sulfide-bearing equilibria are approached, the f_{H_2}, f_{H_2O}, and f_{H_2S} drop to very low values. Although f_{H_2}, f_{H_2O}, and f_{H_2S} can be arbitrary values below the stability lines for FQIPo (f_{H_2}) or FQMPo (f_{H_2O} and f_{H_2S}), only certain univariant-invariant reactions are stable over certain temperature ranges, as shown in Table 10.

Whitney (1984) calculated the fugacities of sulfurous

→

Fig. 9. Log f_i-T phase diagrams for the Fe-Si-O-H-S system at 2 kbar. (**a**) O_2, (**b**) S_2, (**c**) SO_2, (**d**) H_2, (**e**) H_2O, (**f**) H_2S. The sulfide out dashed lines illustrate the upper limits of stabilities for the pyrite- and pyrrhotite-bearing assemblages. Since the uppermost stabilities for the pyrite- and pyrrhotite-bearing assemblages correspond to the highest f_{O_2}, f_{S_2}, and f_{SO_2} and lowest f_{H_2}, f_{H_2O}, and f_{H_2S}, the sulfide out dashed lines are drawn only on the plots for (**a**) f_{O_2}, (**b**) f_{S_2}, and (**c**) f_{SO_2}.

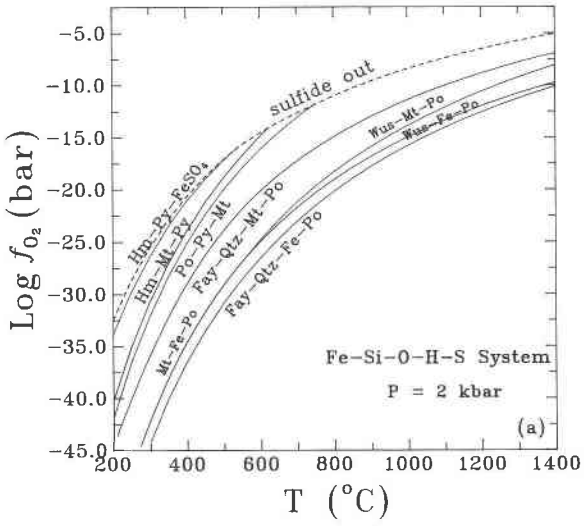
Log f_{O_2} (bar)
T (°C)
sulfide out
Hm–Py–FeSO$_4$
Hm–Mt–Py
Po–Py–Mt
Mt–Fe–Po
Fay–Qtz–Mt–Po
Fay–Qtz–Fe–Po
Wus–Mt–Po
Wus–Fe–Po
Fe–Si–O–H–S System
P = 2 kbar
(a)

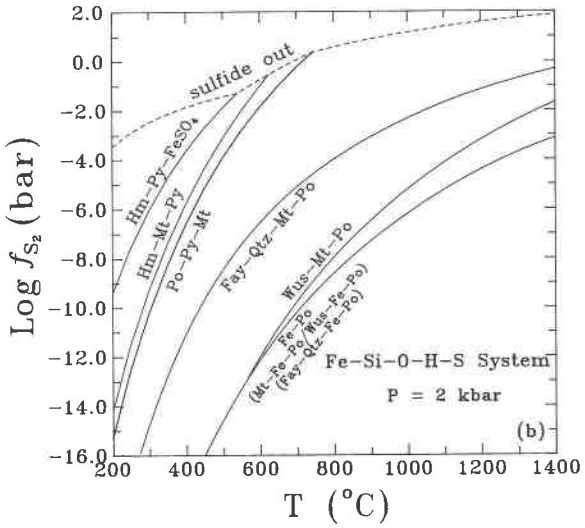
Log f_{S_2} (bar)
T (°C)
sulfide out
Hm–Py–FeSO$_4$
Hm–Mt–Py
Po–Py–Mt
Fay–Qtz–Mt–Po
Wus–Mt–Po
Fe–Po
(Mt–Fe–Po)
(Wus–Fe–Po)
(Fay–Qtz–Fe–Po)
Fe–Si–O–H–S System
P = 2 kbar
(b)

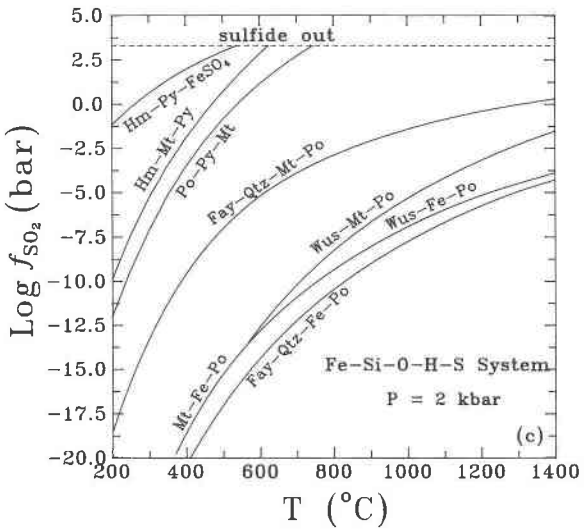
Log f_{SO_2} (bar)
T (°C)
sulfide out
Hm–Py–FeSO$_4$
Hm–Mt–Py
Po–Py–Mt
Fay–Qtz–Mt–Po
Wus–Mt–Po
Wus–Fe–Po
Fay–Qtz–Fe–Po
Mt–Fe–Po
Fe–Si–O–H–S System
P = 2 kbar
(c)

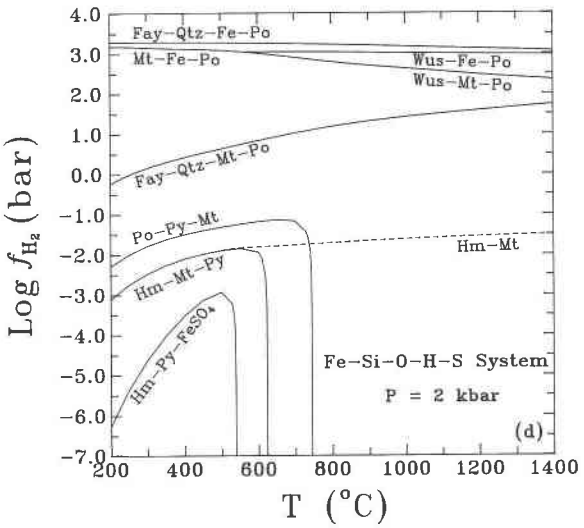
Log f_{H_2} (bar)
T (°C)
Fay–Qtz–Fe–Po
Mt–Fe–Po
Wus–Fe–Po
Wus–Mt–Po
Fay–Qtz–Mt–Po
Po–Py–Mt
Hm–Mt
Hm–Mt–Py
Hm–Py–FeSO$_4$
Fe–Si–O–H–S System
P = 2 kbar
(d)

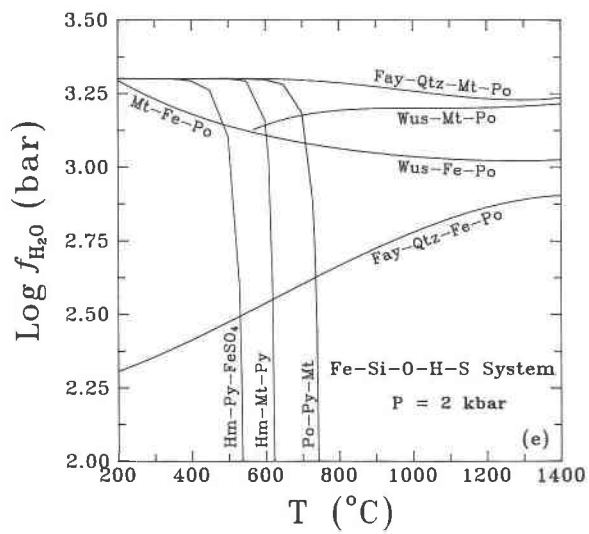
Log f_{H_2O} (bar)
T (°C)
Fay–Qtz–Mt–Po
Mt–Fe–Po
Wus–Mt–Po
Wus–Fe–Po
Fay–Qtz–Fe–Po
Hm–Py–FeSO$_4$
Hm–Mt–Py
Po–Py–Mt
Fe–Si–O–H–S System
P = 2 kbar
(e)

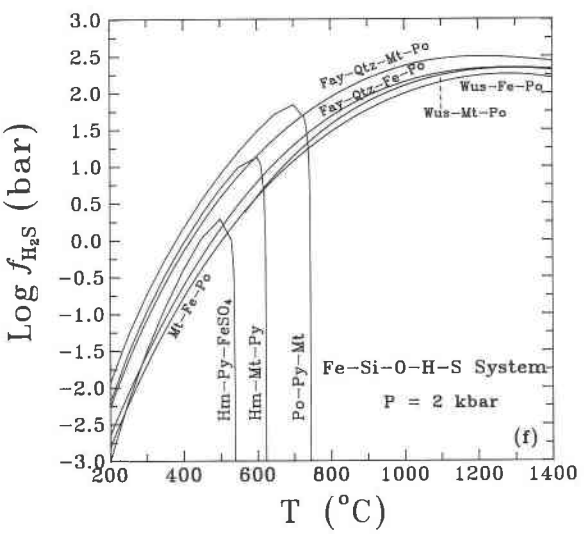
Log f_{H_2S} (bar)
T (°C)
Fay–Qtz–Mt–Po
Fay–Qtz–Fe–Po
Wus–Fe–Po
Wus–Mt–Po
Mt–Fe–Po
Hm–Py–FeSO$_4$
Hm–Mt–Py
Po–Py–Mt
Fe–Si–O–H–S System
P = 2 kbar
(f)

gases (S_2, SO_2, H_2S) of pyrrhotite-bearing assemblages under magmatic conditions, using some simplified formulations in the Fe-S_2-O_2-SiO_2 system. The calculated results presented here (six invariant O-/S-buffering assemblages PPMW, HMPyW, HPyFSW, FQMPoW, FQIPoW, MIWPoW as well as univariant O-bearing assemblages FQMW, HMW, FQIW, MWIW) may be used to understand the phase equilibria in the pyrrhotite/silicate-bearing magmas or hydrothermal processes. At a pressure of 2 kbar, for instance, when the temperature is 600 °C, the f_{O_2}, f_{S_2}, f_{SO_2}, f_{H_2}, f_{H_2O}, and f_{H_2S} of pyrrhotite-bearing silicic magmas are between those of PPMW and of FQMPoW. When the temperature increases to 900 °C, the f_{O_2}, f_{S_2}, f_{SO_2}, f_{H_2}, and f_{H_2S} of pyrrhotite-bearing silicic magmas change to the ranges between those of upper limit for MPoW and of FQMPoW.

Conclusions

The supercritical multicomponent C-H-O-S fluid model is shown to be a useful tool in calculating f_{O_2}-f_{H_2}-f_{S_2} buffers and phase equilibria involving Fe oxides, silicates, and sulfides. Most of the available experimental data on phase equilibria are consistent with the calculated results. The calculated phase diagrams and the tabulated data extend the P-T range of the experimentally determined buffers for geological applications. The theoretical phase diagrams and fluid proportions in the Fe-Si-O-H-S system are useful in understanding the magmatic, metamorphic, and hydrothermal geochemical processes.

Acknowledgments

The author thanks S.K. Saxena for advice. The critical reviews and constructive suggestions from U. Mader, M.S. Ghiorso, and an anonymous reviewer were of great help in improving the manuscript. Financial support was provided by the Swedish Natural Science Research Council (NFR).

References cited

Akimoto, S. (1972) The system MgO-FeO-SiO_2 at high pressures and temperatures—Phase equilibria and elastic properties. Tectonophysics, 13, 167–187.

Akimoto, S., Matsui, Y., and Syono, Y. (1976) High-pressure crystal chemistry of orthosilicates and the formation of the mantle transition zone. In R.G.J. Strens, Ed., Physics and chemistry of minerals and rocks, p. 327–363. Wiley, London.

Ariya, S.M., Morozova, M.P., Stolyarova, T.A., and Selezneva, L.N. (1966) Enthalpy of Fe sulfides (FeS_{1+x}) formation. Zhournal Phisicheskoj Khimii, 40, 1604–1607 (in Russian).

Arnold, R.G. (1958) Pyrrhotite-pyrite equilibrium relations between 325 and 743 °C. Ph.D. dissertation, Princeton University, Princeton, New Jersey.

——— (1962) Equilibrium relations between pyrrhotite and pyrite from 325 to 743 °C. Economic Geology, 75, 72–90.

Arnórsson, S. (1985) Gas pressure in geothermal systems. Chemical Geology, 49, 319–328.

Barin, I., and Knacke, O. (1978) Thermochemical properties of inorganic substances, 981 p. Springer-Verlag, New York.

Barker, W.W., and Parks, T.C. (1986) The thermodynamic properties of pyrrhotite and pyrite: A re-evaluation. Geochimica et Cosmochimica Acta, 50, 2185–2194.

Barton, P.B. (1970) Sulfide petrology. Mineralogical Society of America Special Paper 3, 187–198.

Barton, P.B., and Skinner, B.J. (1979) Sulfide mineral stabilities. In H.L. Barnes, Ed., Geochemistry of hydrothermal ore deposits (2nd edition), p. 278–403. Wiley, New York.

Barton, P.B., and Toulmin, P. (1964) The electrum-tarnish method for determination of fugacity of sulfur in laboratory sulfide systems. Geochimica et Cosmochimica Acta, 28, 619–640.

——— (1966) Phase relations involving sphalerite in Fe-Zn-S system. Economic Geology, 61, 815–849.

Bény, C., Guilhaumou, N., and Touray, J.C. (1982) Native-sulphur-bearing fluid inclusions in the CO_2-H_2S-H_2O-S system—Microthermometry and Raman microprobe (MOLE) analysis—Thermochemical interpretations. Chemical Geology, 37, 113–127.

Bugli, G., Abello, L., and Pannetier, G. (1972) Enthalpy of formation of nonstoichiometric ferrous sulfides $Fe_{1-x}S$. Bulletin de la Société Chimique de France, 2, 497–501 (in French).

Burt, D.M. (1971) Some phase equilibria in the system Ca-Fe-Si-C-O. Carnegie Institution of Washington Year Book, 70, 185–188.

——— (1972) Silicate-sulfide equilibria in Ca-Fe-Si skarn deposits. Carnegie Institution of Washington Year Book, 71, 450–457.

——— (1974) Sulfide-silicate reactions in skarn base-metal deposits (abs.). Proceedings of the Fourth IAGOD Symposium, vol. 3, p. 160–161. International Association on the Genesis of Ore Deposits, Varna, Bulgaria.

Burton, J.C. (1978) Experimental and mineralogical studies of skarn silicates, 155 p. Ph.D. thesis, University of Tennessee, Knoxville, Tennessee.

Burton, J.C., Taylor, L.A., and Chou, I.-M. (1982) The f_{O_2}-T and f_{S_2}-T stability relations of hedenbergite and of hedenbergite-johannsenite solid solutions. Economic Geology, 77, 764–783.

Chatterjee, N. (1987) Evaluation of thermodynamic data on Fe-Mg olivine, orthopyroxene, spinel and Ca-Fe-Mg-Al garnet. Geochimica et Cosmochimica Acta, 51, 2515–2525.

——— (1989) An internally consistent thermodynamic data base on minerals. Ph.D. thesis, City University of New York, New York.

Chipman, J., and Marshall, S. (1940) The equilibrium FeO + H_2 = Fe + H_2O at temperatures up to the melting point of iron. Journal of the American Chemical Society, 62, 299–305.

Chou, I.-M. (1978) Calibration of oxygen buffers at elevated P and T using the hydrogen fugacity sensor. American Mineralogist, 63, 690–703.

——— (1986) Permeability of precious metals to hydrogen at 2 kb total pressure and elevated temperatures. American Journal of Science, 286, 638–658.

Chou, I.-M., and Cygan, G.L. (1990) Quantitative redox control and measurement in hydrothermal experiments. Geochemical Society Special Publication, 2, 3–15.

Craig, J.R., and Scott, S.D. (1974) Sulfide phase equilibria. In Mineralogical Society of America Short Course Notes, 1, CS1–CS110.

Crerar, D.A., Susak, N.J., Borcsik, M., and Schwartz, S. (1978) Solubility of the buffer assemblage pyrite-pyrrhotite-magnetite in NaCl solutions from 200 to 350 °C. Geochimica et Cosmochimica Acta, 42, 1427–1437.

D'Amore, F., and Panichi, C. (1980) Evaluation of deep temperatures of hydrothermal systems by a new gas geothermometer. Geochimica et Cosmochimica Acta, 44, 549–556.

Darken, L.S. (1948) Melting points of iron oxides on silica: Phase equilibria in the system Fe-Si-O as a function of gas composition and temperature. Journal of the American Chemical Society, 70, 2046–2053.

Darken, L.S., and Gurry, R.W. (1945) The system iron-oxygen. I. The wüstite field and related equilibria. Journal of the American Chemical Society, 67, 1398–1412.

——— (1946) The system iron-oxygen. II. Equilibrium and the thermodynamics of liquid oxide and other phases. Journal of the American Chemical Society, 68, 798–816.

Eriksson, G. (1975) Thermodynamic studies of high temperature equilibria. XII. SOLGASMIX a computer program for calculation of equilibrium compositions in multiphase systems. Chemica Scripta, 8, 100–103.

Eriksson, G., and Fredriksson, M. (1983) A solid state EMF study of the pyrrhotite-magnetite equilibrium in the temperature interval 850 to 1275 K. Metallurgical Transactions B, 14B, 459–464.

Eugster, H.P. (1957) Heterogeneous reactions involving oxidation and reduction at high pressures and temperatures. The Journal of Chemical Physics, 26, 1760.

Eugster, H.P., and Wones, D.R. (1962) Stability relations of the ferruginous biotite, annite. Journal of Petrology, 3, 82–125.

Fei, Y., and Saxena, S.K. (1986) A thermodynamic data base for phase equilibria in the system Fe-Mg-Si-O at high pressure and temperature. Physics and Chemistry of Minerals, 13, 311–324.

Fei, Y., Saxena, S.K., and Navrotsky, A. (1990) Internally consistent thermodynamic data and equilibrium phase relations for compounds in the system MgO-SiO_2 at high pressure and high temperature. Journal of Geophysical Research, 95, 6915–6928.

Frantz, J.D., and Eugster, H.P. (1973) Acid-base buffers: Use of Ag + AgCl in the experimental control of solution equilibria at elevated pressures and temperatures. American Journal of Science, 273, 268–286.

Froese, E., and Gunter, A. (1976) A note on the pyrrhotite-sulfur vapor equilibrium. Economic Geology, 71, 1589–1594.

Gamble, R.P. (1978) The sulfidation of andradite and hedenbergite: An experimental study of skarn-ore genesis, 226 p. Ph.D. thesis, Yale University, New Haven, Connecticut.

——— (1982) An experimental study of sulfidation reactions involving andradite and hedenbergite. Economic Geology, 77, 784–797.

Giletti, B.J., Yund, R.A., and Lin, T.J. (1968) Sulfur vapor pressure of pyrite-pyrrhotite (abs.). Economic Geology, 63, 702.

Guilhaumou, N., Velde, B., and Bény, C. (1984) Raman microprobe analysis of gaseous inclusion in diagenetically recrystallized calcites. Bulletin de Minéralogie, 107, 193–202.

Guillermet, A.F., and Gustafson, P. (1985) An assessment of the thermodynamic properties and the (P-T) phase diagram of iron. High Temperatures–High Pressure, 16, 591–619.

Haas, J.L. (1988) Recommended standard electrochemical potentials and fugacities of oxygen for solid buffers and thermodynamic data in the system iron-silicon-oxygen, nickel-oxygen, and copper-oxygen. Preliminary report of January 17, 1988, to the CODATA Task Group on Chemical Thermodynamic Tables. U.S. Geological Survey, Reston, Virginia.

Haas, J.L., and Robie, R.A. (1973) Thermodynamic data for wüstite, $Fe_{0.947}O$, magnetite, Fe_3O_4 and hematite, Fe_2O_3. Eos, 54, 483.

Haggerty, S.E. (1976) Opaque mineral oxides in terrestrial igneous rocks. In Mineralogical Society of America Reviews in Mineralogy, 3, Hg101–Hg300.

Hemingway, B.S. (1990) Thermodynamic properties for bunsenite, NiO, magnetite, Fe_3O_4, and hematite, Fe_2O_3, with comments on selected oxygen buffer reactions. American Mineralogist, 75, 781–790.

Hewitt, D.A. (1978) A redetermination of the fayalite-magnetite-quartz equilibrium between 650 and 850 °C. American Journal of Science, 278, 715–724.

Holland, H.D. (1956a) Some applications of thermodynamic data to problems of ore deposits. I. Stability relations among the oxides, sulfides, sulfates and carbonate of ore and gangue minerals. Economic Geology, 54, 184–233.

——— (1956b) Some applications of thermodynamic data to problems of ore deposits. II. Mineral assemblages and the composition of ore-forming fluids. Economic Geology, 60, 1101–1166.

Holland, T., and Powell, R. (1990) An enlarged and updated internally consistent thermodynamic dataset with uncertainties and correlations: The system K_2O-Na_2O-CaO-MgO-MnO-FeO-Fe_2O_3-Al_2O_3-TiO_2-SiO_2-C-H_2-O_2. Journal of Metamorphic Geology, 8, 89–124.

Hutcheon, I. (1978) Calculation of metamorphic pressure using the sphalerite-pyrrhotite-pyrite equilibrium. American Mineralogist, 63, 87–95.

JANAF (1985) Thermodynamic tables. Journal of Physical and Chemical Reference Data, 14 (suppl 1), 1842.

Janecky, D.R., Seyferied, W.E., Jr., and Berndt, M.E. (1986) Fe-O-S redox reactions and kinetics in hydrothermal systems (abs.). Fifth International Symposium on Water-Rock Interaction, p. 282–285. Reykjavik, Iceland.

Kishima, N. (1986) Simultaneous determination of molecular hydrogen, sulfide, and sulfate in solution samples from experimental hydrothermal systems. Analytical Chemistry, 58, 1255–1258.

——— (1989) A thermodynamic study on the pyrite-pyrrhotite-magnetite-water system at 300–500 °C with relevance to the fugacity/concentration quotient of aqueous H_2S. Geochimica et Cosmochimica Acta, 53, 2143–2155.

Kishima, N., and Sakai, H. (1984) Fugacity-concentration relationship of dilute hydrogen in water at elevated temperature and pressure. Earth and Planetary Science Letters, 67, 79–86.

Kissin, S.A., and Scott, S.D. (1982) Phase relations involving pyrrhotite below 350 °C. Economic Geology, 77, 1739–1754.

Kleman, M. (1965) Proprietes thermodynamiques du protoxyde de fer sous forme solide. Application des resultats experimentaux au trace du diagramme d'equilibre. Mémoires Scientifiques de la Revue de Metallurgie, 26, 457–469.

Kullerud, G., and Yoder, H.S. (1959) Pyrite stability relations in the Fe-S system. Economic Geology, 54, 533–572.

Liebermann, R.C., and Schreiber, E. (1968) Elastic constants of polycrystalline hematite as a function of pressure to 3 kilobars. Journal of Geophysical Research, 73, 6585–6590.

Mao, H.K., Bassett, W.B., and Takahashi, T. (1967) Effect of pressure on crystal structure and lattice parameters of iron up to 300 kbar. Journal of Applied Physics, 38, 272–276.

Mao, H.K., Takahashi, T., Bassett, W.A., Kinsland, G.L., and Merrill, L. (1974) Isothermal compression of magnetite to 320 kbar and pressure-induced phase transformation. Journal of Geophysical Research, 79, 1165–1170.

Mills, K.C. (1974) Thermodynamic data for inorganic sulphides, selenides and tellurides, 843 p. Butterworth, London.

Mironova, O.F., Naumov, V.B., and Salazkin, A.N. (1973) Gas-liquid inclusions containing H_2S in quartz from East Transbaykalia. Geochemical International, 10, 1350–1356.

Myers, J., and Eugster, H. (1983) The system Fe-Si-O: Oxygen buffer calibrations to 1500 K. Contributions to Mineralogy and Petrology, 82, 75–90.

Norton, F.J. (1955) Dissociation pressures of iron and copper oxides. General Electric Research Laboratory Report, no. 55-RL-1248.

Powell, R. (1983) Thermodynamic mixing properties of pyrrhotite. Mineralogical Magazine, 47, 437–440.

Rau, H. (1976) Energetics of defect formations and interaction in pyrrhotite $Fe_{1-x}S$ and its homogeneity range. Journal of Physical Chemistry of Solids, 37, 425–429.

Raymahashay, B.C., and Holland, H.D. (1968) Composition of aqueous solutions in equilibrium with sulfides and oxides of iron at 350 °C. Science, 162, 895–896.

Rizzo, H.F., Gordon, R.S., and Cutler, I.B. (1969) The determination of phase boundaries and thermodynamic functions in the iron-oxygen system by EMF measurements. Journal of the Electrochemical Society, 116, 266–274.

Robie, R.A., and Waldbaum, D.R. (1968) Thermodynamic properties of minerals and related substances at 298.15 K (25 °C) and one atmosphere (1.013 bars) pressure and at higher temperatures. U.S. Geological Survey Bulletin 1259, 256 p.

Robie, R.A., Hemingway, B.S., and Fisher, J.R. (1978) Thermodynamic properties of minerals and related substances at 298.15 K and 1 bar (10^5 pascals) pressure and at higher temperatures. U.S. Geological Survey Bulletin, 1452, 456 p.

Robie, R.A., Finch, C.B., and Hemingway, B.S. (1982) Heat capacity and entropy of fayalite (Fe_2SiO_4) between 5.1 and 383 K: Comparison of calorimetric and equilibrium values for the QFM buffer reaction. American Mineralogist, 67, 463–469.

Roedder, E. (1971) Fluid inclusion studies on the porphyry-type ore deposits at Bingham, Utah, Butte, Montana, and Climax, Colorado. Economic Geology, 66, 98–120.

Saxena, S.K., and Eriksson, G. (1983) Theoretical computation of mineral assemblages in pyrolite and lherzolite. Journal of Petrology, 24, 538–555.

——— (1985) Anhydrous phase equilibria in Earth's upper mantle. Journal of Petrology, 26, 1–13.

——— (1986) Chemistry of the formation of the terrestrial planets. In S.K. Saxena, Ed., Chemistry and physics of terrestrial planets. Advances in physical geochemistry, vol. 6, p. 30–105. Springer-Verlag, New York.

Saxena, S.K., and Fei, Y. (1987a) Fluid at crustal pressures and temper-

atures. 1. Pure species. Contributions to Mineralogy and Petrology, 95, 370–375.
——— (1987b) High pressure and high temperature fluid fugacities. Geochimica et Cosmochimica Acta, 51, 783–791.
——— (1988a) Fluid mixtures in the C-H-O system at high pressure and temperature. Geochimica et Cosmochimica Acta, 52, 505–512.
——— (1988b) The pressure-volume-temperature equation of hydrogen. Geochimica et Cosmochimica Acta, 52, 1195–1196.
Saxena, S.K., Sykes, J., and Eriksson, G. (1986) Phase equilibria in the pyroxene quadrilateral. Journal of Petrology, 27, 843–852.
Saxena, S.K., Chatterjee, N., Fei, Y., and Shen, G. (1992) An assessment of thermodynamics of oxides and silicates. Advances in physical geochemistry, vol. 11, 250 p. Springer-Verlag, New York.
Schneeberg, E.P. (1973) Sulfur fugacity measurements with the electrochemical cell $Ag|AgI|Ag_{2+x}S$, f_{S_2}. Economic Geology, 68, 507–517.
Scott, S.D. (1973) Experimental calibration of the sphalerite geobarometer. Economic Geology, 68, 466–474.
Shi, P., and Saxena, S.K. (1992) Thermodynamic modeling of C-H-O-S fluid system. American Mineralogist, 77, 1038–1049.
Skinner, B.J. (1966) Thermal expansion. Geological Society of America Memoirs, 97, 75–96.
Soga, N. (1968) The temperature and pressure derivatives of isotropic sound velocities of a-quartz. Journal of Geophysical Research, 73, 827–829.
Spry, P.G., and Scott, S.D. (1986) The stability of zincian spinels in sulfide systems and their potential as exploration guides for metamorphosed massive sulfide deposits. Economic Geology, 81, 1446–1463.
Stolyarova, T.A., and Bezman, N.I. (1976) Enthalpies of formation of monoclinic pyrrhotite $Fe_{0.877}S$. Zhournal Phisicheskoj Khimii, 50, 559 (in Russian).
Sumino, Y. (1979) The elastic constants of Mn_2SiO_4, Fe_2SiO_4 and Co_2SiO_4 and the elastic properties of olivine group minerals at high temperature. Journal of Physical Earth, 27, 209–238.
Sundman, B. (1991) An assessment of the Fe-O system. Journal of Phase Equilibria, 12, 127–140.
Sundman, B., Jansson, B., and Andersson, J.O. (1985) The thermo-calc databank system. Calphad, 9, 153–190.
Suzuki, I., Seya, K., Takei, H., and Sumino, Y. (1981) Thermal expansion of fayalite, Fe_2SiO_4. Physics and Chemistry of Minerals, 7, 60–63.
Swaroop, B., and Wagner, J.B. (1967) On the vacancy concentrations of wüstite near the p to n transition. Transactions of the Metallurgical Society of AIME, 239, 1215–1218.
Syono, Y., Akimoto, S., and Matsui, Y. (1971) High pressure transformations in zinc silicates. Journal of Solid State Chemistry, 3, 369–380.
Taylor, R.W., and Schmalzried, H. (1964) The free energy of formation of some titanates, silicates, and magnesium aluminate from measurements made with galvanic cells involving solid electrolytes. Journal of Physical Chemistry, 68, 2444–2449.
Toulmin, P., and Barton, P.B. (1964) A thermodyanmic study of pyrite and pyrrhotite. Geochimica et Cosmochimica Acta, 28, 641–671.
Ulmer, P., and Luth, R.W. (1991) The graphite-COH fluid equilibrium in P-T-f_{O_2} space: An experimental determination to 30 kbar and 1600 °C. Contributions to Mineralogy and Petrology, 106, 265–272.
Weast, R.C., Melvin, J.A., and Beyer, W.H. (1988) CRC handbook of chemistry and physics (69th edition). CRC Press, Boca Raton, Florida.
Whitney, J.S. (1984) Fugacities of sulfurous gases in pyrrhotite-bearing silicic magmas. American Mineralogist, 69, 69–78.
Williams, R.J. (1971) Reaction constants in the system Fe-MgO-SiO_2-O_2 at 1 atm between 900 and 1300 °C: Experimental results. American Journal of Science, 270, 334–360.
Wones, D.R., and Gilbert, M.C. (1969) The fayalite-magnetite-quartz assemblage between 600 °C and 800 °C. American Journal of Science, 267A, 480–488.
Wood, S.A., Crerar, D.A., and Borcsik, M.P. (1987) Solubility of the assemblage pyrite-pyrrhotite-magnetite-sphalerite-galena-gold-stibnite-bismuthinite-argentite-molybdenite in H_2O-NaCl-CO_2 solutions from 200 to 350 °C. Economic Geology, 82, 1864–1887.

Manuscript received October 30, 1991
Manuscript accepted May 4, 1992

ERRATUM

Comparative liquidus equilibria of hypersthene-normative basalts at low pressure, by John Longhi (v. 76, p. 785–800). There are sets of parentheses missing from the equation for Qtz{Wo} in the caption for Figure 3 and from the equation for Opx{Ol} in the caption for Figure 4. The proper form for Qtz{Wo} is

$$\text{Qtz}\{\text{Wo}\} = [2\text{SiO}_2 - (\text{FeO} + \text{MgO} + \text{MnO} + 2\text{Fe}_2\text{O}_3) - 2\text{CaO} - 2\text{Al}_2\text{O}_3 - 10(\text{K}_2\text{O} + \text{Na}_2\text{O})]/\Sigma.$$

The proper form for Opx{Ol} is

$$\text{Opx}\{\text{Ol}\} = 3[2\text{SiO}_2 - (\text{FeO} + \text{MgO} + \text{MnO} + 2\text{Fe}_2\text{O}_3) - 2\text{CaO} - 2\text{Al}_2\text{O}_3 - 10(\text{K}_2\text{O} + \text{Na}_2\text{O})]/\Sigma.$$

There is also a single parenthesis missing from the equation for Qtz{Pl} in the caption for Figure 5. The proper form is

$$\text{Qtz}\{\text{Pl}\} = [2\text{SiO}_2 - (\text{FeO} + \text{MgO} + \text{MnO} + 2\text{Fe}_2\text{O}_3) - 2\text{Al}_2\text{O}_3 - 2\text{CaO} - 10(\text{K}_2\text{O} + \text{Na}_2\text{O})]/\Sigma.$$